LETTER

doi:10.1038/nature13305

SOX2 controls tumour initiation and cancer stem-cell functions in squamous-cell carcinoma

Soufiane Boumahdi[1], Gregory Driessens[1]*, Gaelle Lapouge[1]*, Sandrine Rorive[2,3], Dany Nassar[1], Marie Le Mercier[2], Benjamin Delatte[4], Amélie Caauwe[1], Sandrine Lenglez[1], Erwin Nkusi[1], Sylvain Brohée[5], Isabelle Salmon[2,3], Christine Dubois[1], Veronique del Marmol[6], Francois Fuks[4], Benjamin Beck[1] & Cédric Blanpain[1,7]

Cancer stem cells (CSCs) have been reported in various cancers, including in skin squamous-cell carcinoma (SCC)[1–4]. The molecular mechanisms regulating tumour initiation and stemness are still poorly characterized. Here we find that *Sox2*, a transcription factor expressed in various types of embryonic and adult stem cells[5,6], was the most upregulated transcription factor in the CSCs of squamous skin tumours in mice. SOX2 is absent in normal epidermis but begins to be expressed in the vast majority of mouse and human pre-neoplastic skin tumours, and continues to be expressed in a heterogeneous manner in invasive mouse and human SCCs. In contrast to other SCCs, in which *SOX2* is frequently genetically amplified[7], the expression of SOX2 in mouse and human skin SCCs is transcriptionally regulated. Conditional deletion of *Sox2* in the mouse epidermis markedly decreases skin tumour formation after chemical-induced carcinogenesis. Using green fluorescent protein (GFP) as a reporter of *Sox2* transcriptional expression (SOX2–GFP knock-in mice), we showed that SOX2-expressing cells in invasive SCC are greatly enriched in tumour-propagating cells, which further increase upon serial transplantations. Lineage ablation of SOX2-expressing cells within primary benign and malignant SCCs leads to tumour regression, consistent with the critical role of SOX2-expressing cells in tumour maintenance. Conditional *Sox2* deletion in pre-existing skin papilloma and SCC leads to tumour regression and decreases the ability of cancer cells to be propagated upon transplantation into immunodeficient mice, supporting the essential role of SOX2 in regulating CSC functions. Transcriptional profiling of SOX2–GFP-expressing CSCs and of tumour epithelial cells upon *Sox2* deletion uncovered a gene network regulated by SOX2 in primary tumour cells *in vivo*. Chromatin immunoprecipitation identified several direct SOX2 target genes controlling tumour stemness, survival, proliferation, adhesion, invasion and paraneoplastic syndrome. We demonstrate that SOX2, by marking and regulating the functions of skin tumour-initiating cells and CSCs, establishes a continuum between tumour initiation and progression in primary skin tumours.

Skin SCC is the second most frequent skin cancer and affects more than 500,000 new patients per year throughout the world[8]. Recently, different groups have identified CSCs or tumour-propagating cells (TPCs) expressing a high level of CD34 from primary mouse SCC induced by 9,10-dimethyl-1,2-benzanthracene (DMBA)/2-otetradecanoyl phorbol-13-acetate (TPA) treatment that have a higher capacity than other tumour cells to reform secondary tumours upon transplantation into immunodeficient mice and possess higher long-term self-renewal capacity[1–4]. Very little is known about the mechanisms that regulate cutaneous CSC functions.

To define the intrinsic mechanisms that regulate CSC functions in skin tumours, we determined which transcription factors are differentially expressed between $CD34^+$ and $CD34^-$ $Epcam^+$ tumour epithelial cells (TECs) (Lin^-Epcam^+) in benign papillomas and malignant SCCs. *Sox2*, a transcription factor expressed in a great variety of stem cells[5] and genetically amplified in different cancers, including SCCs from lung and oesophagus[7], was the most upregulated transcription factor expressed in $CD34^+$ TECs from skin papillomas[3]. Quantitative reverse transcription polymerase chain reaction (qRT–PCR) showed that *Sox2* messenger RNA was indeed highly upregulated in $CD34^+$ TECs, and even further upregulated in $CD34^+$ TECs of SCCs (Fig. 1a). Using SOX2–GFP knock-in mice[9], which express GFP under the endogenous regulatory region of *Sox2*, we found that SOX2 expression was absent in the normal epidermis (Fig. 1b), with the exception of in Merkel cells, as previously reported[10,11]. However, upon drug treatment that induced skin hyperproliferation (retinoic acid, TPA, DMBA or DMBA/TPA), focal expression of SOX2–GFP is detected mostly in suprabasal cells of hyperplastic lesions (Fig. 1b and Extended Data Fig. 1). Nonetheless, no SOX2 protein expression is observed at this stage (Extended Data Fig. 1h), possibly owing to the low level of SOX2 expression. Immunostaining and fluorescence-activated cell sorting (FACS) analysis revealed that SOX2 was expressed in a heterogeneous manner at the mRNA and protein level in more than 80% of primary mouse papillomas and SCCs (Fig. 1c–e and Extended Data Fig. 2a), preferentially but not exclusively expressed in a subset of $CD34^+$ TECs (Fig. 1c, d and Extended Data Fig. 2b–d). SOX2 is expressed with a similar frequency and heterogeneity in DMBA/TPA- and Kras(G12D)-induced papilloma and SCCs (Fig. 1e and Extended Data Fig. 2), suggesting that the cellular origin of tumour cells and the mutational heterogeneity are not the primary determinant of SOX2 expression. Immunostaining of a collection of human specimens revealed that SOX2 was expressed in the majority of pre-neoplastic skin lesions—termed actinic keratoses (29/40 patients)—and continued to be expressed in a heterogeneous manner in the majority of invasive SCCs (25/39 patients) (Fig. 1f and Extended Data Fig. 3).

SOX2 is genetically amplified in SCCs from different tissues such as the oesophagus[7], where SOX2 is naturally expressed[6]. However, no genetic amplification of *Sox2* was detected in mouse and human skin tumour cells (Fig. 1g, h and Extended Data Fig. 4). *Ezh1/2* deletion, which prevents the deposition of H3K27me3 repressive histone marks, increases SOX2 expression in the developing skin epidermis[12]. Using chromatin immunoprecipitation (ChIP) experiments, we found that the *Sox2* promoter was associated with repressive histone marks in normal skin and with active histone marks in SCCs (Fig. 1i, j). Altogether, these data indicate that *Sox2* is not genetically amplified but transcriptionally and/or epigenetically regulated during skin tumour initiation in both mice and humans.

To determine whether SOX2 expression during the initial stages of skin tumour initiation is required for tumour formation, we investigated the rate and number of tumours formed upon DMBA/TPA treatment in *Sox2*-deficient epidermis (K14Cre:$SOX2^{fl/fl}$; ref. 13) (Extended Data

[1]Université Libre de Bruxelles, IRIBHM, Brussels B-1070, Belgium. [2]Department of Pathology, Erasme Hospital, Université Libre de Bruxelles, Brussels B-1070, Belgium. [3]DIAPATH—Center for Microscopy and Molecular Imaging (CMMI), Gosselies B-6041, Belgium. [4]Laboratory of Cancer Epigenetics, Université Libre de Bruxelles, Brussels B-1070, Belgium. [5]Machine Learning Group, Computer Science Department, Faculté des Sciences, Université Libre de Bruxelles, Brussels B-1050, Belgium. [6]Department of Dermatology, Erasme Hospital, Université Libre de Bruxelles, Brussels B-1070, Belgium. [7]WELBIO, Université Libre de Bruxelles, Brussels B-1070, Belgium.
*These authors contributed equally to this work.

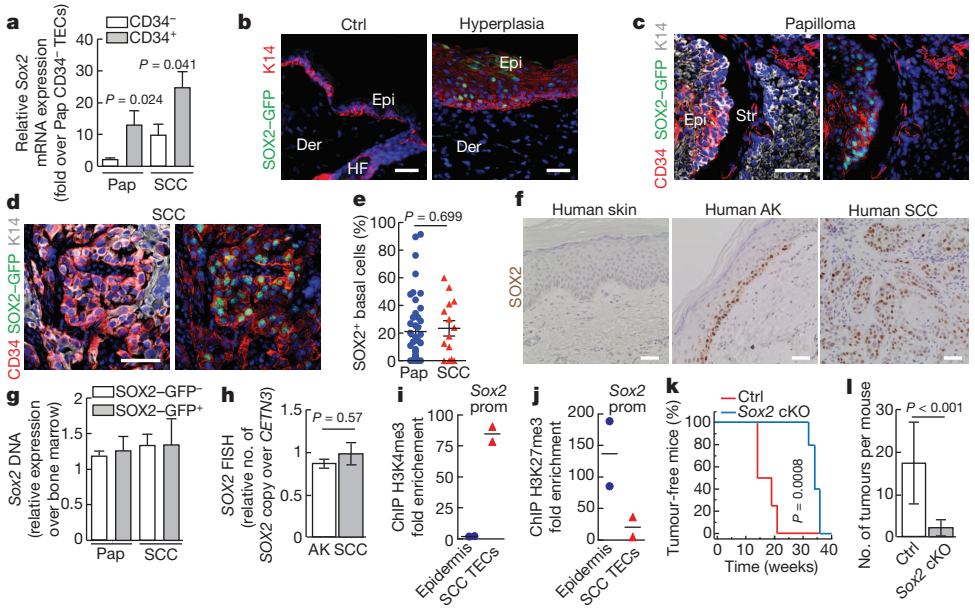

Figure 1 | SOX2 is expressed in pre-neoplastic skin tumours, invasive SCCs and regulates skin tumour initiation. **a**, qRT–PCR analysis of *Sox2* mRNA expression in FACS-isolated CD34$^+$ and CD34$^-$ TECs ($n = 5$ tumours for each group). Pap, papilloma. **b**–**d**, Immunostaining of SOX2–GFP, CD34 and K14 showed the presence of SOX2–GFP$^+$ cells in hyperplasic skin and in benign and malignant tumours. Ctrl, control; Der, dermis; Epi, epidermis; HF, hair follicle; Str, tumour stroma. **e**, Quantification of the proportion of basal SOX2$^+$ TECs within benign and malignant tumours measured by immunofluorescence ($n \geq 1{,}600$ total cell counted in $n = 14$ tumours from 14 mice). **f**, Immunostaining for SOX2 in human normal skin, actinic keratosis (AK) and invasive SCC. **g**, Quantification of *Sox2* DNA copy number by qRT–PCR of FACS-isolated SOX2–GFP$^+$ and SOX2–GFP$^-$ TECs. Data were normalized relatively to the house keeping genes *Gabra* and β-actin in tumour cells and in bone-marrow cells (germline DNA) of each mouse ($n = 3$ tumours from 3 different mice in each group). **h**, Quantification of *SOX2* DNA copy number by fluorescence *in situ* hybridization (FISH) in human actinic keratosis and SCC. The data were normalized to the number of CETN3 dots ($n \geq 50$ nuclei counted per AK ($n = 3$) and per SCC ($n = 5$)). **i**, **j**, ChIP of H3K4me3 (**i**) and H3K27me3 (**j**) at the *Sox2* promoter (prom) in normal epidermis and SCC TECs ($n = 2$ skins and $n = 2$ primary SCCs). Fold change represents the percentage of input recovered after immunoprecipation with the antibody of interest normalized over the percentage of input recovered with beads alone. **k**, Percentage of control and *Sox2* conditional knockout (cKO) mice presenting with skin tumours over time ($n = 5$ mice in each group). **l**, Average number of tumours per mice 40 weeks after tumour initiation (control $n = 7$; *Sox2* conditional knockout $n = 5$ mice). **b**, **c**, **d**, **f**, Hoechst nuclear staining is represented in blue; scale bars, 50 μm. Data represent the mean and standard error of the mean (s.e.m.).

Fig. 5a, b). Although conditional *Sox2* deletion has no effect on the development and homeostasis of the skin epidermis (Extended Data Fig. 5c, d), it delayed the appearance of skin tumours by several months and decreased the number of tumours by almost tenfold as compared with littermate controls (Fig. 1k, l and Extended Data Fig. 5e, f), indicating that SOX2 has an essential role during the early stages of skin tumour initiation.

At present, the gold standard assay to assess CSC potential is the transplantation of limiting dilutions of highly purified prospectively identified cancer cell populations into immunodeficient mice to assess their ability to form secondary tumours[14,15]. Transplantation of SOX2–GFP$^+$ TECs from invasive SCC (Extended Data Fig. 6a) showed that they had a much greater ability to reform secondary tumours compared with Epcam$^+$ SOX2–GFP$^-$ and total Epcam$^+$ TECs (Fig. 2a, b), and this difference further increased during serial transplantation (Fig. 2c). To assess the respective enrichment of TPCs in cells expressing CD34 and SOX2, we compared the efficiency of secondary tumour formation after the transplantation of all four Epcam$^+$ TEC populations (SOX2–GFP$^+$/CD34$^+$, SOX2–GFP$^+$/CD34$^-$, SOX2–GFP$^-$/CD34$^+$ and SOX2–GFP$^-$/CD34$^-$) (Extended Data Fig. 6b). Interestingly, SOX2–GFP$^+$ CD34$^+$ double-positive cells showed the greatest ability to reform secondary tumours (Fig. 2d). SOX2–GFP$^+$/CD34$^-$ TECs, although much less efficient than SOX2–GFP$^+$/CD34$^+$ TECs, were more efficient than SOX2–GFP$^-$ cells irrespective of CD34 expression (Fig. 2d). These results further support the idea that SOX2 is the primary determinant of TPC frequency and identify SOX2$^+$/CD34$^+$ TECs as the most efficient subpopulation of TPCs in skin SCC.

Grafted SOX2–GFP$^+$ TECs reformed tumours that recapitulated the histology of the primary SCCs, with a concomitant increase in the proportion of SOX2-expressing cells with serial transplantation (Extended Data Fig. 6a, c). The proportion of SOX2–GFP$^+$ cells after serial transplantation of all Epcam$^+$ TECs increased from 25% in the primary tumours to 80% after the second transplantation (Extended Data Fig. 6d–f), supporting the selective growth advantage of SOX2–GFP$^+$ TECs. The few tumours that arise from the transplantation of a high number of SOX2–GFP$^-$ TECs contained SOX2–GFP$^+$ and SOX2–GFP$^-$ cells (Extended Data Fig. 6g–j), suggesting that upon transplantation, rare SOX2–GFP$^-$ cells can revert back to SOX2–GFP$^+$ cells to sustain tumour propagation, but that this transition is very inefficient.

The higher proportion of TPCs in SOX2$^+$ cells indicates that these cells may represent the cells that feed tumour growth within their natural environment. To investigate this possibility, we evaluated the impact of SOX2 cell lineage ablation on tumour growth (Extended Data Fig. 7a, b). Administering tamoxifen to SOX2CreER:Rosa-DTA mice with skin tumours led to the complete regression of most benign tumours (Fig. 2e, f and Extended Data Fig. 7c–d) and a strong regression of invasive SCCs (Fig. 2g and Extended Data Fig. 7e), suggesting that SOX2 marks a population of tumour cells necessary for tumour growth and maintenance *in vivo*.

To gain further insights into the molecular mechanisms that regulate CSC function, we transcriptionally profiled SOX2–GFP$^+$ TECs. Interestingly, SOX2–GFP$^+$ cells were enriched for genes known to be expressed by CSCs from other tumours or regulating stem cells in other systems (for example, *Hmga2* (refs 16, 17), *Ptprz1* (refs 18, 19), *Cd133* (also known as *Prom1*) (ref. 20), *Cd34* (refs 1–3), *Igf2bp2* (ref. 21) and *Vegfa* (ref. 3)) (Fig. 2h), proliferation (for example, *Ccnd1/2* and *Met*), cell survival and autophagy, cell adhesion (for example, *Itga3*), invasion, DNA damage response and resistance to therapy (for example, *Chek2*, *Aurka/b*, *Mgmt* and *Abcb1*), transcription factors (for example, *Pitx1* and *Etv5*) and chromatin regulators (for example, *Scmh1*) (Extended Data Fig. 8). In addition, a significant fraction of the genes upregulated

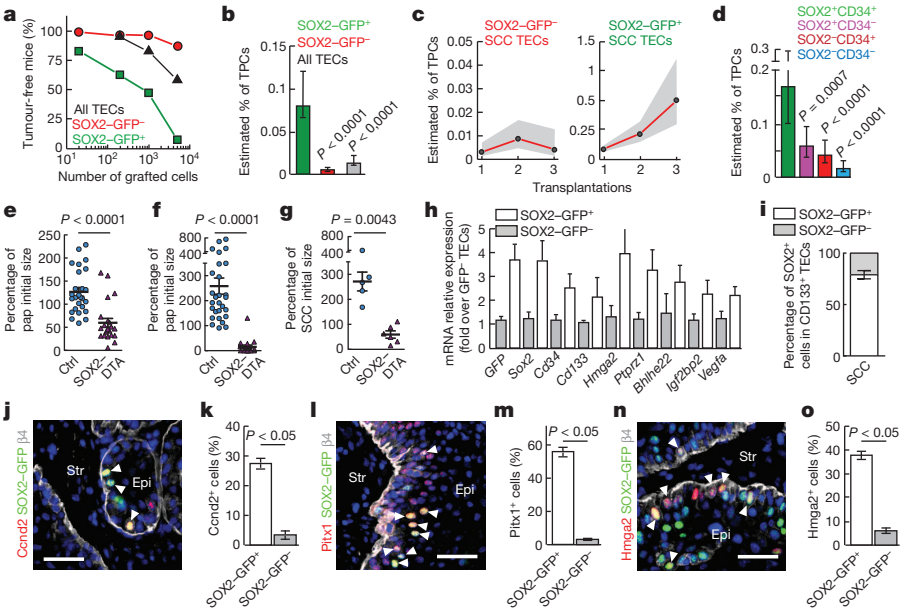

Figure 2 | SOX2 marks skin SCC tumour-propagating cells. **a**, Graph representing the percentage of tumour-free mice 5 weeks after subcutaneous injection of different dilutions of SOX2–GFP$^+$, SOX2–GFP$^-$ and all Epcam$^+$ TECs into immunodeficient mice. **b**, Estimated percentage of TPCs in SOX2–GFP$^+$ and SOX2–GFP$^-$ TECs after the first transplantation using the extreme limiting dilution analysis[30] ($n = 30$ grafted tumours per dilution from five independent SCCs). **c**, Graph representing the estimated percentage of TPCs in SOX2–GFP$^+$ and SOX2–GFP$^-$ TECs during serial transplantations. **d**, Estimated percentage of TPCs in different TEC populations after the first transplantation ($n = 15$ grafted tumours per dilution from five independent SCCs). **e**, Quantification of the variation in tumour size 1 week after the beginning of tamoxifen administration (intraperitoneal (i.p.)) in control (Ctrl) and SOX2–DTA mice ($n > 22$ tumours from 4 different mice in each group). **f**, **g** Size of papilloma (pap; **f**) and SCC (**g**) 2 weeks after the beginning of tamoxifen administration (topical) in control and SOX2–DTA mice ($n > 18$ papillomas and $n > 5$ SCCs from 3 mice in each group). **h**, qRT–PCR analysis of stemness genes in SOX2–GFP$^+$ and SOX2–GFP$^-$ TECs ($n = 3$ tumours from 3 different mice for each group). **i**, FACS quantification of the percentage of SOX2–GFP$^+$ cells in CD133$^+$ TECs ($n = 5$ SCCs). **j**–**o**, Immunostaining and quantification of the expression of Ccnd2 (**j**, **k**), Pitx1 (**l**, **m**) and Hmga2 (**n**, **o**) together with β4-integrin (β4) in SOX2–GFP$^+$ and SOX2–GFP$^-$ TECs ($n \geq 2{,}578$ total cell counted per marker in $n = 5$ tumours from 3 different mice). Epi, epithelium; Str, tumour stroma. Hoechst nuclear staining is represented in blue; scale bars, 50 μm. Data represent the mean and s.e.m. (except for transplantation assay: error bars (**b**, **d**) and grey area (**c**) represent the 95% confidence interval of the estimation).

in SOX2–GFP$^+$ TECs were also preferentially expressed by embryonic epidermal cells (Extended Data Fig. 8), indicating that SOX2$^+$ CSCs reactivate a genetic program expressed in the embryonic epidermis. Using FACS analysis and immunostaining, we confirmed the preferential expression of selected genes in SOX2–GFP$^+$ CSCs, such as those controlling tumour proliferation (for example, *Ccnd2*) (Fig. 2j, k), *Pitx1*, a transcription factor expressed in human oral SCCs[22] (Fig. 2l, m), cell adhesion (for example, *Itga3*) or associated with tumour stemness (for example, *Hmga2*, *Igf2bp2* and *Cd133*) (Fig. 2i, n, o and Extended Data Fig. 8).

SOX2 knockdown using short hairpin RNA (shRNA) in various cancer cell lines decreased tumour cell growth *in vitro* and/or *in vivo*

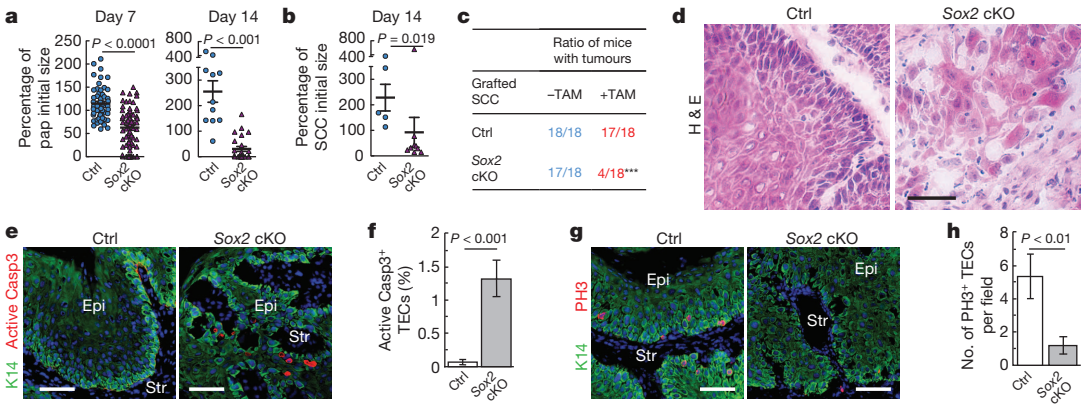

Figure 3 | SOX2 is essential for skin tumour maintenance. **a**, Tumour size 1 week (left) after the beginning of tamoxifen administration (12.5 mg i.p.) ($n \geq 66$ tumours from 8 different mice) and 2 weeks (right) after the beginning of topical tamoxifen administration (control $n = 11$ papillomas (pap); *Sox2* conditional knockout $n = 24$ papillomas (pap) from 4 different mice in each group). **b**, Carcinoma size 2 weeks after the beginning of topical tamoxifen administration ($n > 5$ SCCs from 3 different mice) **c**, Table summarizing the frequency of secondary tumours after subcutaneous injection of 50,000 total SCC cells from control (Ctrl) and *Sox2* conditional knockout (cKO) animals after tamoxifen (TAM) administration ($n = 6$ grafted points per SCC). ***$P \leq 0.001$ (as compared with TAM-induced control). **d**, Haematoxylin and eosin (H&E) staining of control and *Sox2* conditional knockout tumours. **e**–**h**, Immunostaining and quantification of TEC (K14$^+$) apoptosis (active Casp3$^+$) ($n = 7$ papillomas from 4 different mice) (**e**, **f**) and proliferation (phospho-histone H3$^+$) ($n = 9$ papillomas from 3 different mice) (**g**, **h**) after *Sox2* deletion. Epi, epithelium; Str, tumour stroma. Hoechst nuclear staining is represented in blue; scale bars, 50 μm. Data represent the mean and s.e.m.

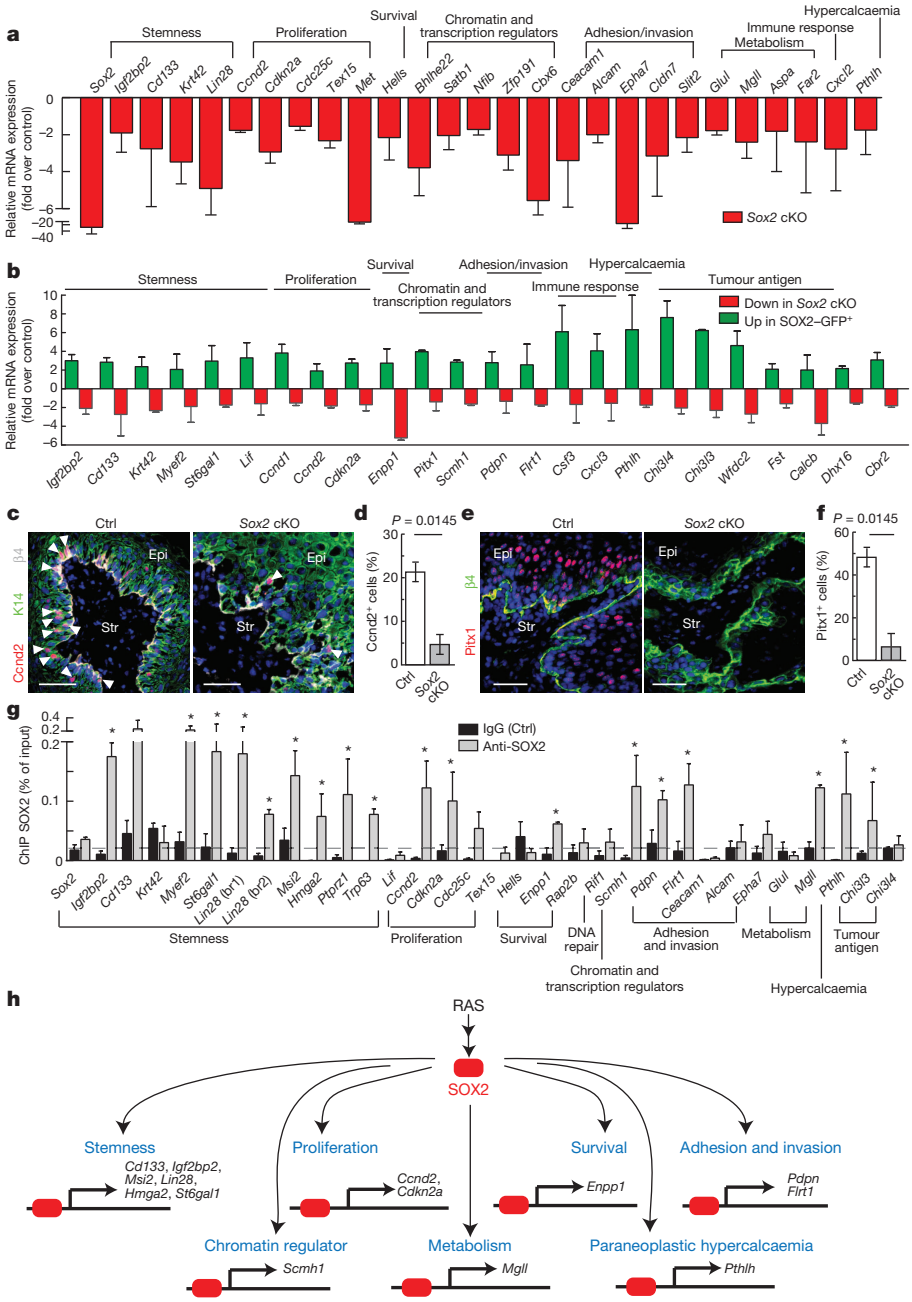

Figure 4 | SOX2 controls a gene network that regulates tumour proliferation and stemness. **a**, qRT–PCR analysis of selected genes from different functional categories after *Sox2* deletion ($n = 3$ tumours from 3 different mice for each genotype). **b**, Microarray analysis of genes upregulated (Up) in the SOX2$^+$ CSC signature and downregulated (Down) in the SOX2-regulated gene signature, illustrating the genes positively controlled by SOX2 in CSCs ($n = 3$ different tumours from 3 mice in each group). Data represent the mean and s.e.m. of replicate arrays. **c–f**, Immunostaining and quantification of the expression of Ccnd2 (**c**, **d**) and Pitx1 (**e**, **f**) in K14 TECs after *Sox2* deletion ($n \geq 1{,}743$ total cells counted in $n = 3$ papillomas from 3 different mice). Ctrl, control; cKO, conditional knockout; Epi, epithelium; Str, tumour stroma. Hoechst nuclear staining is represented in blue; scale bars, 50 μm. **g**, SOX2 direct target genes in primary SCCs assessed by ChiP-qPCR analysis. Data represent the mean and s.e.m. of the percentage of input recovered after ChiP with SOX2 antibody or with the IgG at known[28] or putative SOX2-binding sites in the promoter region of the genes indicated. The dashed line represents the percentage of input for a negative control region (Trpm7) ($n = 3$ tumours from 3 different mice). br1/2, binding region1/2. *$P \leq 0.05$. **h**, Model of SOX2 functions in skin CSCs.

after their transplantation into immunodeficient mice[23]. However, so far no study has demonstrated the requirement for SOX2 expression to sustain the growth of established primary tumours. To determine whether SOX2 regulates tumour maintenance and CSC functions *in vivo* in primary tumours, we performed conditional deletion of *Sox2* in pre-existing skin tumours (Extended Data Fig. 9a, b). Tamoxifen administration over 2 weeks to K14CreER:SOX2$^{fl/fl}$ mice with skin tumours led to complete regression of the vast majority of benign papillomas (Fig. 3a and Extended Data Fig. 9c) and induced a strong regression in the size of malignant SCCs (Fig. 3b). Consistent with the absence of SOX2 expression in a minor fraction of skin tumours, a few tumours did not regress after *Sox2* deletion (Fig. 3a, b). These data show the essential role of SOX2 for primary tumour growth and maintenance *in vivo* in benign and malignant SCCs. Conditional deletion of *Sox2* in SCC cells after their transplantation into immunodeficient mice decreased their TPC capacity by more than 80% (Fig. 3c), further supporting the notion that SOX2 regulates tumour stemness in primary skin SCCs. *Sox2* deletion induced major changes in papilloma tumour-cell shape, which were much bigger and flatter (Fig. 3d), markedly increased apoptosis and decreased cell proliferation in papilloma and SCC (Fig. 3e–h and Extended Data Fig. 10), leading to a decrease in the production of differentiated TECs (Extended Data Fig. 9e).

To determine the molecular mechanisms by which SOX2 regulates tumour maintenance and cancer-cell functions in primary mouse skin tumours, we induced *Sox2* deletion in pre-existing tumour cells and performed microarray and qRT–PCR of TECs in the presence or absence of SOX2 (SOX2-regulated gene signature) (Fig. 4a). Functional analysis of these differentially expressed genes revealed that SOX2 regulates directly and/or indirectly the expression of a number of genes involved in many critical aspects of cancer functions[24] (Fig. 4a and Extended Data Fig. 9g).

To understand more precisely the mechanisms by which SOX2 regulates tumour stemness in SOX2–GFP$^+$ CSCs, we defined the genes preferentially upregulated in SOX2–GFP$^+$ cells and downregulated upon *Sox2* deletion ($P = 6 \times 10^{-9}$) (Fig. 4b, Extended Data Fig. 9h and Supplementary Table 1). These genes included CSC markers (for example,

Cd133)[20], genes that control tumour stemness in other malignancies (for example, *Igf2bp2*)[21], cell proliferation (for example, *Ccnd2*), survival (for example, *Enpp1*) and inflammation (for example, *Cxcl3*), transcription and chromatin remodelling (for example, *Pitx1* and *Scmh1*), as well as *Pthlh*, the gene responsible for paraneoplastic hypercalcaemia[25] (Fig. 4b). Immunostaining of papilloma in which *Sox2* had been acutely deleted confirmed that *Ccnd2*, a gene controlling cell proliferation, *Pitx1*, a transcription factor expressed in SCCs[22], and *Pdpn*, a mucin-like glycoprotein expressed in a variety of SCCs associated with poor prognosis[26], were strongly decreased upon *Sox2* deletion (Fig. 4c–f and Extended Data Fig. 9f). Interestingly, a fraction of the downregulated genes following conditional deletion of *Sox2* in TECs are also found to be directly and indirectly regulated by SOX2 in embryonic stem cells[27,28] and in brain tumour cell lines[29] (Extended Data Fig. 9h–j and Supplementary Tables 1–3), suggesting that SOX2 may regulate some common mechanisms across a range of stem cells including CSCs. Using ChIP-qPCR, we found that many genes downregulated upon *Sox2* deletion and controlling tumour proliferation and metabolism, and associated with stemness in other systems, such as *Ccnd2*, *Igf2bp2*, *Cd133*, *Scmh1*, *St6gal1*, *Mgll*, *Pdpn*, *Msi2*, *Lin28* and *Trp63* were bound by SOX2 in primary SCC (Fig. 4g). Other SOX2-binding sites in *Glul*, *Hells* and *Chi3l4* (also known as *Chil4*), as well as in *Lif* and *Krt42*—which are directly bound by SOX2 in embryonic stem cells (Supplementary Tables 1, 2)—were not bound by SOX2 in primary SCCs (Fig. 4g), indicating the specificity of the SOX2-regulated genes in SCC. Our molecular analysis of SOX2 function in tumour cells shows that SOX2 directly regulates the expression of key genes involved in cancer-cell proliferation, stemness, chromatin regulation, metabolism and paraneoplastic hypercalcaemia in primary skin tumours *in vivo* (Fig. 4h).

We identify SOX2 as marking a continuum in skin carcinogenesis from tumour-initiating cells to the regulation of CSC functions in invasive cancer (Fig. 4h). Considering the broad diversity of cancers expressing SOX2, the functions and downstream target genes of SOX2 uncovered in primary skin tumours are likely to be relevant for other cancers, as well as for the development of novel strategies targeting CSCs.

METHODS SUMMARY

DMBA/TPA chemical carcinogenesis, measurement of tumour size, transplantation assays, immunostaining, RNA extraction and qRT–PCR were performed as previously described[4]. ChIP, Comparative genomic hybridization (CGH) array, FISH, microarray analysis and statistical analysis were performed as described in Methods.

Online Content Any additional Methods, Extended Data display items and Source Data are available in the online version of the paper; references unique to these sections appear only in the online paper.

Received 20 August 2013; accepted 31 March 2014.
Published online 8 June 2014.

1. Malanchi, I. *et al.* Cutaneous cancer stem cell maintenance is dependent on β-catenin signalling. *Nature* **452,** 650–653 (2008).
2. Schober, M. & Fuchs, E. Tumor-initiating stem cells of squamous cell carcinomas and their control by TGF-β and integrin/focal adhesion kinase (FAK) signaling. *Proc. Natl Acad. Sci. USA* **108,** 10544–10549 (2011).
3. Beck, B. *et al.* A vascular niche and a VEGF–Nrp1 loop regulate the initiation and stemness of skin tumours. *Nature* **478,** 399–403 (2011).
4. Lapouge, G. *et al.* Skin squamous cell carcinoma propagating cells increase with tumour progression and invasiveness. *EMBO J.* **31,** 4563–4575 (2012).
5. Sarkar, A. & Hochedlinger, K. The Sox family of transcription factors: versatile regulators of stem and progenitor cell fate. *Cell Stem Cell* **12,** 15–30 (2013).
6. Arnold, K. *et al.* Sox2^{+} adult stem and progenitor cells are important for tissue regeneration and survival of mice. *Cell Stem Cell* **9,** 317–329 (2011).
7. Bass, A. J. *et al. SOX2* is an amplified lineage-survival oncogene in lung and esophageal squamous cell carcinomas. *Nature Genet.* **41,** 1238–1242 (2009).
8. Alam, M. & Ratner, D. Cutaneous squamous-cell carcinoma. *N. Engl. J. Med.* **344,** 975–983 (2001).
9. Ellis, P. *et al.* SOX2, a persistent marker for multipotential neural stem cells derived from embryonic stem cells, the embryo or the adult. *Dev. Neurosci.* **26,** 148–165 (2004).
10. Laga, A. C. *et al.* Expression of the embryonic stem cell transcription factor SOX2 in human skin: relevance to melanocyte and Merkel cell biology. *Am. J. Pathol.* **176,** 903–913 (2010).
11. Driskell, R. R., Giangreco, A., Jensen, K. B., Mulder, K. W. & Watt, F. M. Sox2-positive dermal papilla cells specify hair follicle type in mammalian epidermis. *Development* **136,** 2815–2823 (2009).
12. Bardot, E. S. *et al.* Polycomb subunits Ezh1 and Ezh2 regulate the Merkel cell differentiation program in skin stem cells. *EMBO J.* **32,** 1990–2000 (2013).
13. Taranova, O. V. *et al.* SOX2 is a dose-dependent regulator of retinal neural progenitor competence. *Genes Dev.* **20,** 1187–1202 (2006).
14. Beck, B. & Blanpain, C. Unravelling cancer stem cell potential. *Nature Rev. Cancer* **13,** 727–738 (2013).
15. Meacham, C. E. & Morrison, S. J. Tumour heterogeneity and cancer cell plasticity. *Nature* **501,** 328–337 (2013).
16. Copley, M. R. *et al.* The Lin28b–let-7–Hmga2 axis determines the higher self-renewal potential of fetal haematopoietic stem cells. *Nature Cell Biol.* **15,** 916–925 (2013).
17. Nishino, J., Kim, I., Chada, K. & Morrison, S. J. Hmga2 promotes neural stem cell self-renewal in young but not old mice by reducing $p16^{Ink4a}$ and $p19^{Arf}$ Expression. *Cell* **135,** 227–239 (2008).
18. Himburg, H. A. *et al.* Pleiotrophin regulates the retention and self-renewal of hematopoietic stem cells in the bone marrow vascular niche. *Cell Rep.* **2,** 964–975 (2012).
19. Soh, B. S. *et al.* Pleiotrophin enhances clonal growth and long-term expansion of human embryonic stem cells. *Stem Cells* **25,** 3029–3037 (2007).
20. Grosse-Gehling, P. *et al.* CD133 as a biomarker for putative cancer stem cells in solid tumours: limitations, problems and challenges. *J. Pathol.* **229,** 355–378 (2013).
21. Janiszewska, M. *et al.* Imp2 controls oxidative phosphorylation and is crucial for preserving glioblastoma cancer stem cells. *Genes Dev.* **26,** 1926–1944 (2012).
22. Libório, T. N. *et al. In situ* hybridization detection of homeobox genes reveals distinct expression patterns in oral squamous cell carcinomas. *Histopathology* **58,** 225–233 (2011).
23. Liu, K. *et al.* The multiple roles for Sox2 in stem cell maintenance and tumorigenesis. *Cell. Signal.* **25,** 1264–1271 (2013).
24. Hanahan, D. & Weinberg, R. A. Hallmarks of cancer: the next generation. *Cell* **144,** 646–674 (2011).
25. Esbrit, P. Hypercalcemia of malignancy—new insights into an old syndrome. *Clin. Lab.* **47,** 67–71 (2001).
26. Chuang, W. Y., Chang, Y. S., Yeh, C. J., Wu, Y. C. & Hsueh, C. Role of podoplanin expression in squamous cell carcinoma of upper aerodigestive tract. *Histol. Histopathol.* **28,** 293–299 (2013).
27. Masui, S. *et al.* Pluripotency governed by *Sox2* via regulation of *Oct3/4* expression in mouse embryonic stem cells. *Nature Cell Biol.* **9,** 625–635 (2007).
28. Marson, A. *et al.* Connecting microRNA genes to the core transcriptional regulatory circuitry of embryonic stem cells. *Cell* **134,** 521–533 (2008).
29. Fang, X. *et al.* The SOX2 response program in glioblastoma multiforme: an integrated ChIP-seq, expression microarray, and microRNA analysis. *BMC Genomics* **12,** 11 (2011).
30. Hu, Y. & Smyth, G. K. ELDA: extreme limiting dilution analysis for comparing depleted and enriched populations in stem cell and other assays. *J. Immunol. Methods* **347,** 70–78 (2009).

Supplementary Information is available in the online version of the paper.

Acknowledgements We thank our colleagues who provided us with reagents. We also thank the animal house facility of the Université Libre de Bruxelles (ULB) (Erasme campus). C.B. is an investigator of WELBIO. S.Bo., B.B., B.D., S.Br., G.L. and D.N. are supported by a FNRS/FRIA, FNRS and TELEVIE fellowships. G.D. is supported by the Brussels Region through the BB2B program. This work was supported by the FNRS, TELEVIE, BB2B program, the IUAP program, a research grant from the Fondation Contre le Cancer, the ULB foundation, the Fonds Yvonne Boël, the Fonds Gaston Ithier, the foundation Bettencourt Schueller, and a starting grant from the European Research Council.

Author Contributions C.B., S.Bo., G.D. and G.L. designed the experiments and performed data analysis. S.Bo., G.L., G.D., D.N. and B.B. performed all the experiments. V.d.M., S.R., M.L.M. and I.S. collected data and performed the analysis of SOX2 expression and gene amplification on human samples. A.C., E.N., S.L. and C.D. provided technical support. S.Br. performed microarray analysis. B.D. and F.F. performed and analysed ChIP for histone marks. C.B. wrote the manuscript.

Author Information Microarray data have been deposited in the Gene Expression Omnibus under accession numbers GSE55737 and GSE55738. Reprints and permissions information is available at www.nature.com/reprints. The authors declare no competing financial interests. Readers are welcome to comment on the online version of the paper. Correspondence and requests for materials should be addressed to C.B. (Cedric.Blanpain@ulb.ac.be).

METHODS

Mice. NOD/SCID/Il2Rg null mice were obtained from Charles River. SOX2–GFP knock-in[9], $SOX2^{fl/fl}$ (ref. 13), Rosa26-DTA[31], K14Cre[32], K14CreER[33], K19CreER[34], InvCreER[35], Lgr5CreER[36], $Kras^{LSL\text{-}G12D}$ (ref. 37), $p53^{fl/fl}$ (ref. 38) and Sox2CreER[6] mice have been previously described and were provided by E. Fuchs, K. Hochedlinger and B. Hogan, or obtained from Jackson Laboratories.

All mice used in this study were from mixed gender, mixed strains and more than 8 weeks old. For all experiments presented in this study, the sample size was large enough to measure the effect size. No randomization and no blinding were performed in this study.

Mouse colonies were maintained in a certified animal facility in accordance with European guidelines.

DMBA/TPA-induced skin tumours. Mice were treated with DMBA and TPA as previously described[3,4,39].

Kras(G12D)-induced skin tumours. K14CreER:$Kras^{LSL\text{-}G12D}$:$p53^{fl/fl}$, Lgr5CreER:$Kras^{LSL\text{-}G12D}$:$p53^{fl/fl}$, K19CreER:$Kras^{LSL\text{-}G12D}$ and InvCreER:$Kras^{LSL\text{-}G12D}$ mice were treated with tamoxifen as previously described[35]. K14CreER:$Kras^{LSL\text{-}G12D}$:$p53^{fl/fl}$:SOX2-GFP were treated with 2.5 mg of tamoxifen i.p. and then topically with 4-hydroxy-tamoxifen every 2 days.

SOX2–GFP expression in skin hyperplasia. Mice were topically treated with retinoic acid (0.1% in DMSO) and vehicle (DMSO) for 2 weeks or were topically treated with DMBA (1× per week plus 1× acetone), TPA (1× per week plus 1× acetone), DMBA/TPA (1× DMBA plus 1× TPA per week) and vehicle (acetone, 2× per week) for 6 weeks. GFP expression in treated skins was assessed by immunofluorescence on skin sections or by FACS as previously described[40,41].

Measurement of papilloma growth. Skin tumours were measured using a precision calliper, allowing us to discriminate size modifications >0.1 mm. Tumour volumes were measured on the first day of treatment and the day of euthanization with the formula $V = \pi \times (d^2 \times D)/6$, where d is the minor tumour axis and D is the major tumour axis.

ChIP assay

H3K4me3/H3K27me3 ChIP. Normal skin or FACS-isolated TECs from primary SCCs were crosslinked for 10 min at room temperature with 1% formaldehyde in complete medium. The reaction was quenched by addition of 0.125 M glycine and washed twice with 1× cold PBS. ChIP experiments were performed according to the TF ChIP kit (Diagenode) protocol. Briefly, sonication was performed with a bioruptor (Diagenode) to produce chromatin fragments of an average of 300 bp. Two micrograms of mouse monoclonal antibody for H3K4me3 (ab1012; Abcam) or 2 μg of mouse monoclonal antibody for H3K27me3 (ab6002; Abcam) were incubated with chromatin overnight at 4 °C. After extensive washing steps, ChIPed DNA was eluted and reverse-crosslinked overnight at 65 °C, then purified using QIAquick PCR purification kit (Qiagen). Three microlitres of enriched fragmented DNA, 0.5 μM of primers and SYBR Green master mix, was subjected to 40 cycles of PCR using LightCycler 480 II (Roche). Fold change over background was calculated by dividing the percentage of input recovered after immunoprecipitation with the antibody of interest over beads incubated without antibodies. Primers used for the *Sox2* promoter are the following. ChIP anti-H3K27me3 primers: Fwd, ATGGGCTCTGTGGTCAAGTCC; Rev, CCCTGGAGTGGGAGGAAGAG; ChIP anti-H3K4me3 primers: Fwd, GCCTTTGCACCCTTTGGATG; Rev, TCA GGTGTGGCTCAAGGAACC.

SOX2 ChIP. Assays were performed as previously described[28], using the EZ-Magna ChIP kit (Millipore). Briefly, after tumour digestion, 20×10^6 cells were crosslinked with 1% formaldehyde for 10 min at room temperature. The reaction was quenched by addition of 0.125 M glycine and washed twice with 1× cold PBS. Cell pellets were snap frozen in liquid nitrogen. The fixed cells were re-suspended in the lysis buffer. Samples were sonicated with a bioruptor (Diagenode) to produce chromatin fragments of an average of 400 bp. Antibodies used for ChIP included SOX2 (AF2018, R&D) and normal goat IgG control (AB-108-C; R&D). Five micrograms of antibody and 20 μl protein G beads were incubated for 6 h at 4 °C. Sonicated chromatin was incubated with the protein G–antibody complex overnight at 4 °C. After wash and elution from the beads, precipitated immunocomplex was treated with proteinase K and reverse crosslinked overnight at 65 °C. DNA was purified following the manufacturer's recommendations (Millipore).

ChIP DNA was analysed by performing qPCR as described later. Results were analysed by calculating the percentage of input recovered for each DNA region, after ChIP using SOX2 antibody or with the IgG control, and comparing it to the percentage of input recovered for a negative control region (containing no known or putative SOX2-binding site). Sequences of primers used are available in Supplementary Table 4.

Antibodies. The following primary antibodies were used: anti-SOX2 (rabbit 1:100; Abcam), anti-CD34 (rat, clone RAM34, 1:50; BD), anti-β4-integrin (rat, clone 346-11A, 1:200; BD), anti-K10 (polyclonal rabbit, 1:1,000; Covance), anti-K14 (polyclonal chicken, 1:2,000; Covance), anti-active caspase 3 (rabbit, 1:600; R&D), anti-BrDU FITC (rat, 1:50; BD), anti-YFP (polyclonal rabbit, 1:2,000; Invitrogen) or anti-YFP (chicken, 1:2,000; Abcam), anti-Hmga2 (rabbit, 1:500; Santa Cruz), anti-pH3 (rabbit, 1:600; Cell Signaling), anti-Igf2bp2 (rabbit, 1:200; Abcam), anti-Ceacam1 (sheep, 1:50; R&D), anti-Pitx1 (rabbit, 1:50; Novus), anti-Itga3 (goat, 1:50; R&D), anti-Pdpn (hamster, clone RTD4E10, 1:200; Abcam), anti-Ccnd2 (rabbit, 1:200; Proteintech), anti-β-catenin (mouse, 1:1,000; Abcam).

The following secondary antibodies were used: anti-rabbit, anti-rat, anti-goat, anti-chicken, anti-hamster, anti-sheep conjugated to Alexa Fluor-488 (Molecular Probes), to rhodamine Red-X (Jackson ImmunoResearch) or to Cy5 (Jackson ImmunoResearch). Pictures were acquired using Axio Imager M1 Microscope, AxioCamMR3 camera and using Axiovision software (Carl Zeiss).

Immunostaining. All the antibodies described earlier were used on frozen sections. Depending on the antibodies used, the tissues were either embedded in OCT (Tissue Tek) and sections were fixed in 4% PAF for 10 min at room temperature, or tumours were pre-fixed for 2 h in 4% PAF, and embedded in OCT. Samples were sectioned in 4–7 μm sections using CM3050S cryostat (Leica Microsystems GmbH). Nonspecific antibody binding was prevented by blocking with 5% horse serum (HS), 1% BSA and 0.2% Triton X-100 for 1 h at room temperature. Primary antibodies were incubated overnight at 4 °C in blocking buffer. Sections were rinsed three times in PBS and incubated with secondary antibodies diluted at 1:400 for 1 h at room temperature. Nuclei were stained in Hoechst solution (4 mM) and slides were mounted using Glycergel (Dako) supplemented with 2.5% DABCO (Sigma-Aldrich).

The stainings on paraffin sections (for SOX2 antibody) were performed and stained as previously described[41]. Briefly, 5 μm paraffin sections were deparaffinized and rehydrated. The antigen unmasking procedure was performed for 20 min at 98 °C in citrate buffer (pH 6) using the PT module. Endogenous peroxydase was blocked using 3% H_2O_2 (Merck) in methanol (VWR) for 10 min at room temperature. Endogenous avidin and biotin were blocked using the Endogenous Blocking kit (Invitrogen) for 20 min at room temperature. Rabbit anti-SOX2 antibody was incubated overnight at 4 °C. Anti-rabbit biotinylated, Standard ABC kit and ImmPACT DAB (Vector Laboratories) were used for the detection of HRP activity. Slides were then dehydrated and mounted using SafeMount (Labonord).

Image acquisition. Imaging was performed on a Zeiss Axio Imager.M1 (Thornwood) fluorescence microscope with a Zeiss Axiocam MR3 camera for immunofluorescence microscopy and a Zeiss Axioxam MRC5 camera for bright-field microscopy using Axiovision release 4.6 software. Photoshop CS3 (Adobe) was used to adjust brightness, contrast and picture size.

SOX2 copy number in mouse papillomas and SCCs. SOX2–GFP^+ and SOX2–GFP^- TECs were sorted from SOX2–GFP mice bearing papillomas and carcinomas. Bone marrow was harvested for each mouse analysed. DNA extraction on sorted cells and bone marrow cells was performed as described later. qPCR analysis was performed using 2 ng of genomic DNA as a template, using a SYBRGreen mix (Applied Bioscience) and an Agilent Technologies Stratagene Mx3500P real-time PCR system. Analysis of the results was performed using Mxpro software (Stratagene) and relative quantification was performed using the DDCt method with β-actin, *Gabra* and *Gpr15* as internal references. Relative DNA copy number was normalized to the corresponding bone marrow.

Comparative genomic hybridization array (array CGH, Agilent, SurePrint G3, 1M probes) were performed at the Nucleomics core facility, Vlaams Instituut voor Biotechnologie (VIB) (Flanders Institute for Biotechnology), on FACS-isolated TECs from DMBA/TPA-induced SCC and compared to the germline DNA from bone marrow cells of the same mice. DNA was extracted using Qiagen DNeasy blood and tissue kit (catalogue no. 69504) according to the manufacturer's instructions after RNAase A treatment (140 U ml^{-1}) (Qiagen catalogue no. 19101). Data are segmented and normalized in relation to the intensity of their neighbouring probes to detect with high confidence genomic regions that have been amplified or deleted[42,43].

SOX2 expression in human SCCs. Tissue samples were obtained retrospectively from archival formalin-fixed and paraffin-embedded samples from 8 normal skins, 40 actinic keratoses and 39 skin SCCs collected in the Department of Pathology of the Erasme Hospital. All histopathological diagnoses were reviewed and assessed according to the 2006 World Health Organization classification[44,45]. More specifically, tumour differentiation was categorized as 'well', 'moderately' and 'poorly' differentiated according to the degree of anaplasia in the tumour nests. Tumour invasion was noted as 'minimal' if the tumour thickness did not exceed 2 mm and 'large' in tumours greater than 2 mm in thickness[44,45]. For each patient, one paraffin block containing representative tissue was selected for the analysis. The available clinical data were collected for each SCC patient and included age at diagnosis, tumour site, margin status and follow-up characterized in terms of progression-free survival and overall survival.

Five-micrometre-thick sections were subjected to standard immunohistochemistry (IHC) as previously described[46]. The IHC expression was visualized by means of streptavidin-biotin-peroxydase complex kit reagents (BioGenex) using

diaminobenzidine/H_2O_2 as the chromogenic substrate. Counterstaining with haematoxylin concluded the processing. The expression of SOX2 was detected by immunostaining using a rabbit monoclonal anti-SOX2 antibody (ab92494, clone EPR3131, dilution 1/100; Abcam). For each staining, an external positive control was included, as well as a negative control, which entailed replacing the primary antibody with non-immune serum (Dako).

All SOX2 stainings were assessed by a pathologist (S.R.) blinded to the clinicopathological data of the patients. The percentage of cell staining (0%, 1–5%, 5–20%, >20%), the cellular staining localization (nuclear and/or cytoplasmic) and the staining intensities (0–3) were assigned for each case.

The comparison of proportion was carried out using Fisher's test (2 × 2 cases). Survival data were analysed using the standard Kaplan–Meier analysis. Survival curves were compared using the log-rank test. All statistical analyses were carried out using Statistica (Statsoft). A list of the human skin SCCs samples used for these analyses is available in Supplementary Table 5.

SOX2 FISH. FISH was performed on sections of human AKs ($n = 3$) and SCCs ($n = 5$) expressing SOX2. Four-micrometre paraffin tissue sections were treated with the ZytoLight FISH-Tissue Implementation Kit (ZytoVision) according to the manufacturer's instructions. FISH was performed using a green-labelled *SOX2* gene probe in combination with an orange-labelled centromeric probe for chromosome 3 (Zytolight SPEC SOX2/CEN3 Dual Colour Probe; Zytovision). Slides were then counterstained with 125 ng ml^{-1} 4′,6-diamidino-2-phenylindole (DAPI) and the green and orange signals were counted in 50 non-overlapping nuclei per tissue sample. Assessment of *SOX2* amplification status was performed by comparing the number of green signals (SOX2) to the number of orange signals (centromeric region, CETN3). The *SOX2* gene was considered to be amplified when the SOX2/CETN3 ratio was greater than 2.

FACS isolation of TECs. Tumours were digested in collagenase I (Sigma) for 2 h at 37 °C on a rocking plate. Collagenase I activity was blocked by addition of EDTA (5 mM) and then rinsed in PBS supplemented with 2% FCS. After tumour digestion, cells were blocked for 15 min at room temperature in PBS supplemented with 30% FCS. Immunostaining was performed using biotin-conjugated anti-CD34 (clone RAM34, 1:50; BD Pharmingen), biotin-conjugated anti-CD133 (clone 13A4, 1:50; eBiosciences), FITC-conjugated anti-a6-integrin (clone GoH3, 1:50; BD Pharmingen), PE-conjugated anti-CD45 (clone 30F11, 1:50; eBiosciences), PE-conjugated anti CD31 (clone MEC13.3, 1:50; BD Pharmingen), PE-conjugated anti-CD140a (clone APA5, 1:50; eBiosciences), APC-Cy7-conjugated anti-Epcam (clone G8.8, 1:50; Biolegend) by incubation for 30 min on ice. Cells were washed and stained using APC-conjugated streptavidin (BD Pharmingen) for 30 min on ice. Living tumour cells were selected by forward scatter, side scatter, doublet discrimination and by Hoechst dye exclusion. TECs were selected based on the expression of Epcam (Epcam$^+$) and exclusion of CD45, CD31, CD140a (Lin$^-$). FACS analysis was performed using FACSAria and FACSDiva software (BD Biosciences). Sorted cells were collected either in culture medium for *in vivo* transplantation experiments or into lysis buffer for RNA extraction.

Transplantation assays into immunodeficient mice. The different FACS-isolated cell populations (Epcam$^{+/-}$, SOX2–GFP$^{+/-}$ and CD34$^{+/-}$) from SCCs were collected in 4 °C medium. Different dilutions (5,000/1,000/200/20) of Lin$^-$/Epcam$^+$/SOX2–GFP$^+$, Lin$^-$/Epcam$^+$/SOX2–GFP$^-$ TECs resuspended in 50 µl of Matrigel (50 µl, E1270, 970 mg ml^{-1}; Sigma) were injected subcutaneously into NOD/SCID/Il2Rg null mice (Charles River). Technical triplicate injections per mouse were performed. For the transplantation of SCC *Sox2* conditional knockout TECs, 50,000 tumour cells were injected subcutaneously and mice were treated with tamoxifen after transplantation. Secondary tumours were detected by palpation every week and their size monitored until tumours reached 1 cm^3 or when mice presented signs of distress, and the mice were killed.

Estimation of the relative frequency of TPCs. Estimation of the relative frequency of TPCs was performed using the extreme limiting dilution analysis (ELDA) as described[30] and calculated using the ELDA online software (http://bioinf.wehi.edu.au/software/elda/). The statistical *P* value was obtained using a Chi-squared test.

Lineage ablation of SOX2-expressing cells. SOX2CreER:Rosa26-DTA mice and their littermate controls were treated with DMBA/TPA as described earlier. After tumour appearance, mice were injected i.p. with 2.5 mg tamoxifen (Sigma) dissolved in sunflower seed oil or treated topically everyday with 4-hydroxy-tamoxifen (2 mg ml^{-1}) (Sigma) for 2 weeks. Rosa26-DTA littermates were used as controls. Tumours were measured, as described earlier, on the day of injection and 6 and 14 days later to quantify tumour growth.

Conditional deletion of *Sox2* in pre-existing tumour cells. K14CreER:SOX2$^{fl/fl}$ mice and their littermate controls were treated with DMBA/TPA as described earlier. After tumour appearance, mice were injected i.p. with 12.5 mg tamoxifen dissolved in sunflower seed oil (2.5 mg per day over 5 consecutive days) and treated topically everyday with 4-hydroxy-tamoxifen (Sigma) for 2 weeks. Tumours were measured, as described earlier, on the day of injection and 7 and 14 days later to quantify tumour growth.

RNA extraction, DNA extraction and qRT–PCR. The protocol used for RNA extraction on FACS-isolated TECs has been previously described[3]. Briefly, RNA extraction was performed using the RNeasy micro kit (Qiagen) according to the manufacturer's recommendations and DNAase treatment. After nanodrop RNA quantification and analysis of RNA integrity, purified RNA was used to synthesize the first-strand cDNA in a 50 µl final volume, using Superscript II (Invitrogen) and random hexamers (Roche). Control of genomic contaminations was measured for each sample by performing the same procedure with or without reverse transcriptase. qPCR analyses were performed with 2 ng of cDNA as a template, using a SYBRGreen mix (Applied Bioscience) and an Agilent Technologies Stratagene Mx3500P real-time PCR system.

Relative quantitative RNA was normalized using the housekeeping gene β-actin. Primers were designed using Roche Universal ProbeLibrary Assay Design Center (http://lifescience.roche.com/shop/CategoryDisplay?catalogId=10001&tab=&identifier=Universal+Probe+Library#tab-3) and are presented in Supplementary Table 6.

Analysis of the results was performed using Mxpro software (Stratagene) and relative quantification was performed using the DDCt method with β-actin as a reference. The entire procedure was repeated in at least three biologically independent samples.

Microarray analysis. Total RNA was analysed using the mouse whole-genome 430 2.0 array from Affymetrix at the AROS Applied Biotechnology A/S microarray facility. All the results were normalized using fRMA normalization with the R-bioconductor package fRMA[47,48] using standard parameters.

Two different biological replicates from SOX2–GFP$^+$ and SOX2–GFP$^-$ TECs were analysed.

The upregulated or downregulated genes in SOX2–GFP$^+$ versus SOX2–GFP$^-$ TECs (>twofold) provided a list of 689 and 1,013 genes, respectively, which we termed the SOX2–GFP$^+$ CSC signature.

Microarray analysis was performed on FACS-isolated Epcam$^+$ a6$^+$ TECs from three different biological experiments after tamoxifen administration to K14CreER:SOX2$^{fl/fl}$ and control mice. The upregulated or downregulated genes (>1.5 fold) in K14CreER:SOX2$^{fl/fl}$ TECs compared to control TECs provided a list of 373 and 337 genes, respectively, which we termed the SOX2-regulated gene signature.

In order to define the upregulated genes in SOX2–GFP$^+$ TECs versus IFE basal cells[49] and the upregulated genes in E16 basal epidermal cells[50] versus adult IFE basal cells, these microarray data were first all normalized using fRMA with the InSilico DB platform[51] and then compared to each other using Gene-E software (Broad Institute). To determine the genes that are enriched in SOX2–GFP$^+$ TECs compared with normal skin, we screened the data sets for genes absent from the skin (defined with a signal <60) and upregulated in SOX2–GFP$^+$ TECs (>threefold). We analysed this set of genes with the functional annotation clustering tool on DAVID Database[52,53]. To determine the genes that are enriched in E16 basal epidermal cells compared with normal skin, we screened the data sets for genes upregulated with at least threefold difference.

When comparing two sets of genes, the hypergeometric *P* value indicates the probability of observing by chance the same overlap between the query set and the reference set.

Statistics. Statistical and graphical data analyses were performed using Origin 7 (OriginLab) and Prism 5 (Graphpad) software. All experiments shown were replicated at least twice. Data represent mean ± s.e.m. with the exception of TPC frequency data (Fig. 2b–d), which consist of the 95% confidence interval of the estimated percentage. Data were tested for normality using either the D'Agostino and Pearson omnibus normality test or the Kolmogorov–Smrinov test (with Dallal–Wilkinson–Lilliefor *P* value). The variation within each experimental group was estimated to ensure that the variance was similar for groups that were being statistically compared; otherwise we used Welch's correction. Statistical significance was calculated by the Mann–Whitney test when the sample size was small (Figs 1e, h, l, 2e–g and 3a, b), Fisher's exact test for analysis of proportions (Fig. 3c and Extended Data Fig. 3), unpaired *t*-test for unpaired observations with normal distribution (Figs 2k, m, o, 3f, h, 4d, f, g and Extended Data Fig. 8j), paired *t*-test for paired observations with normal distributions (Fig. 1a and Extended Data Fig. 2d), log-rank test for ranked observations (Fig. 1k), Chi-squared test for analysis of proportions when *n* is large (Fig. 2b, d) or analysis of variance for multiple comparisons followed by Tukey test for comparisons of each pair of conditions (Extended Data Fig. 6f) using the Graphpad Prism software, considering $P < 0.05$ as statistically significant. All tests are two-sided.

31. Ivanova, A. *et al. In vivo* genetic ablation by Cre-mediated expression of diphtheria toxin fragment A. *Genesis* **43,** 129–135 (2005).

32. Vasioukhin, V., Bauer, C., Degenstein, L., Wise, B. & Fuchs, E. Hyperproliferation and defects in epithelial polarity upon conditional ablation of α-catenin in skin. *Cell* **104,** 605–617 (2001).
33. Vasioukhin, V., Degenstein, L., Wise, B. & Fuchs, E. The magical touch: genome targeting in epidermal stem cells induced by tamoxifen application to mouse skin. *Proc. Natl Acad. Sci. USA* **96,** 8551–8556 (1999).
34. Means, A. L., Xu, Y., Zhao, A., Ray, K. C. & Gu, G. A. $CK19^{CreERT}$ knockin mouse line allows for conditional DNA recombination in epithelial cells in multiple endodermal organs. *Genesis* **46,** 318–323 (2008).
35. Lapouge, G. *et al.* Identifying the cellular origin of squamous skin tumors. *Proc. Natl Acad. Sci. USA* **108,** 7431–7436 (2011).
36. Barker, N. *et al.* Identification of stem cells in small intestine and colon by marker gene *Lgr5*. *Nature* **449,** 1003–1007 (2007).
37. Tuveson, D. A. *et al.* Endogenous oncogenic $K\text{-}ras^{G12D}$ stimulates proliferation and widespread neoplastic and developmental defects. *Cancer Cell* **5,** 375–387 (2004).
38. Jonkers, J. *et al.* Synergistic tumor suppressor activity of BRCA2 and p53 in a conditional mouse model for breast cancer. *Nature Genet.* **29,** 418–425 (2001).
39. Abel, E. L., Angel, J. M., Kiguchi, K. & DiGiovanni, J. Multi-stage chemical carcinogenesis in mouse skin: fundamentals and applications. *Nature Protocols* **4,** 1350–1362 (2009).
40. Blanpain, C., Lowry, W. E., Geoghegan, A., Polak, L. & Fuchs, E. Self-renewal, multipotency, and the existence of two cell populations within an epithelial stem cell niche. *Cell* **118,** 635–648 (2004).
41. Sotiropoulou, P. A. *et al.* Bcl-2 and accelerated DNA repair mediates resistance of hair follicle bulge stem cells to DNA-damage-induced cell death. *Nature Cell Biol.* **12,** 572–582 (2010).
42. Venkatraman, E. S. & Olshen, A. B. A faster circular binary segmentation algorithm for the analysis of array CGH data. *Bioinformatics* **23,** 657–663 (2007).
43. van de Wiel, M. A. *et al.* CGHcall: calling aberrations for array CGH tumor profiles. *Bioinformatics* **23,** 892–894 (2007).
44. McKee, P. H., Calonje, E. & Granter, S. R. in *Pathology of the Skin with Clinical Correlations* 1199–12092 (Elsevier Mosby, 2008).
45. Philip, E., LeBoit, G. B., Weedom, D. & Sarasin, A. in *WHO Classification of Tumours. Pathology and Genetics of Skin Tumours* 20–25 (World Health Organization, 2006).
46. Rorive, S. *et al.* TIMP-4 and CD63: new prognostic biomarkers in human astrocytomas. *Mod. Pathol.* **23,** 1418–1428 (2010).
47. McCall, M. N., Bolstad, B. M. & Irizarry, R. A. Frozen robust multiarray analysis (fRMA). *Biostatistics* **11,** 242–253 (2010).
48. Gentleman, R. C. *et al.* Bioconductor: open software development for computational biology and bioinformatics. *Genome Biol.* **5,** R80 (2004).
49. Ezhkova, E. *et al.* EZH1 and EZH2 cogovern histone H3K27 trimethylation and are essential for hair follicle homeostasis and wound repair. *Genes Dev.* **25,** 485–498 (2011).
50. Ezhkova, E. *et al.* Ezh2 orchestrates gene expression for the stepwise differentiation of tissue-specific stem cells. *Cell* **136,** 1122–1135 (2009).
51. Coletta, A. *et al.* InSilico DB genomic datasets hub: an efficient starting point for analyzing genome-wide studies in GenePattern, Integrative Genomics Viewer, and R/Bioconductor. *Genome Biol.* **13,** R104 (2012).
52. Huang da, W., Sherman, B. T. & Lempicki, R. A. Bioinformatics enrichment tools: paths toward the comprehensive functional analysis of large gene lists. *Nucleic Acids Res.* **37,** 1–13 (2009).
53. Huang da, W., Sherman, B. T. & Lempicki, R. A. Systematic and integrative analysis of large gene lists using DAVID bioinformatics resources. *Nature Protocols* **4,** 44–57 (2009).

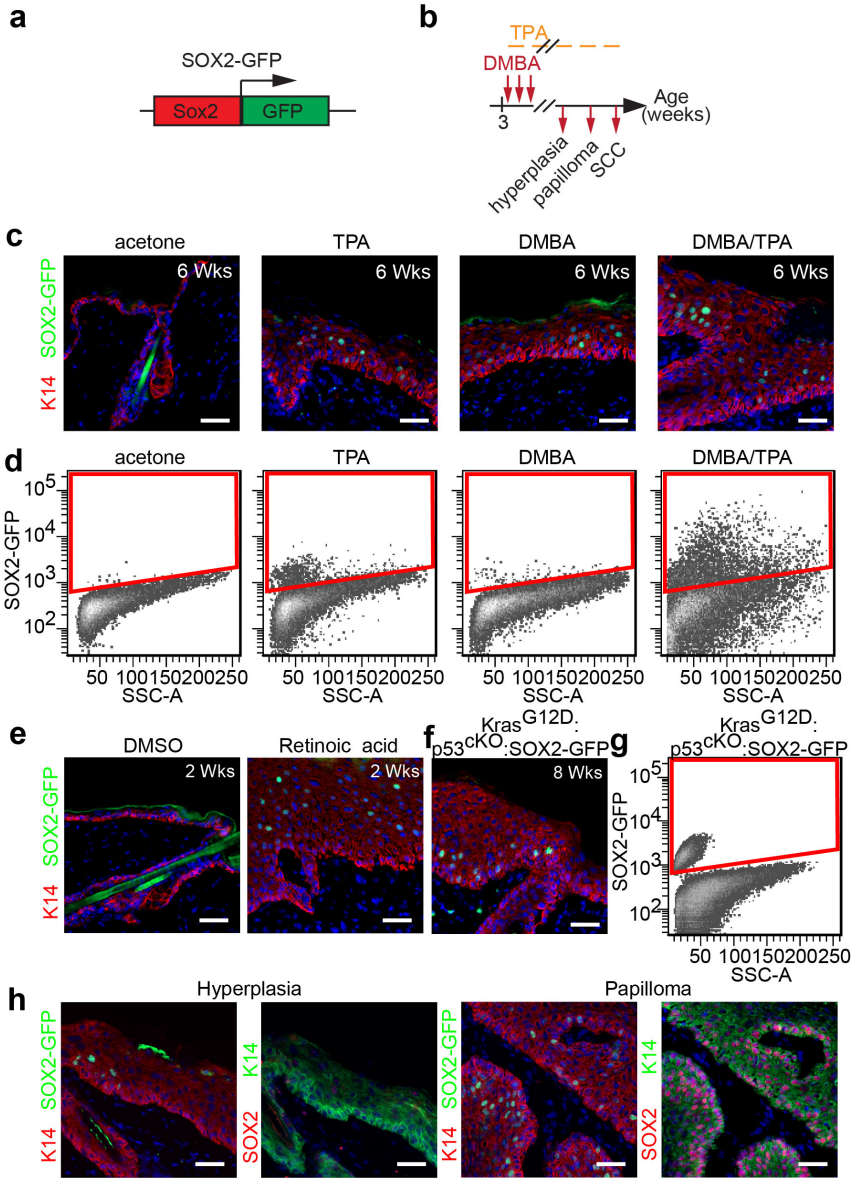

Extended Data Figure 1 | SOX2–GFP expression in skin hyperplasia. **a**, **b**, Genetic strategy (**a**) and experimental design (**b**) used to monitor *Sox2* expression during skin tumorigenesis. **c**, Immunostaining for K14 and GFP in the skin epidermis of SOX2–GFP mice treated for 6 weeks with acetone (Ctrl), TPA, DMBA or DMBA/TPA. **d**, Representative FACS plots of SOX2–GFP expression in the epidermis of mice treated for 6 weeks with acetone (Ctrl), TPA, DMBA or DMBA/TPA. These data show that SOX2–GFP expression is absent in the epidermis of control mice but appears in epidermal hyperplasia during chemical-induced carcinogenesis. **e**, Immunostaining for K14 and GFP in epidermis from SOX2–GFP knock-in mice treated for 2 weeks with DMSO (Ctrl) or retinoic acid. **f**, **g**, Immunostaining for K14 and GFP in epidermal hyperplasia (**f**) and FACS analysis of the skin epidermis (**g**) following Kras(G12D) expression and p53 deletion 8 weeks after tamoxifen administration to K14CreER:Kras^{G12D}:p53^{cKO}:SOX2–GFP mice. These data show that SOX2–GFP is expressed in Kras(G12D)-induced epidermal hyperplasia before tumour formation. **h**, Co-immunostaining for K14 and SOX2–GFP or SOX2 protein in serial sections of SOX2–GFP DMBA/TPA-treated skin. These results show that *Sox2* is transcriptionally upregulated in pathological conditions associated with massive and sustained proliferation of epidermal stem cells. However, although SOX2–GFP is detected in skin hyperplasia, SOX2 protein is only detected in skin tumours. Scale bars, 50 μm.

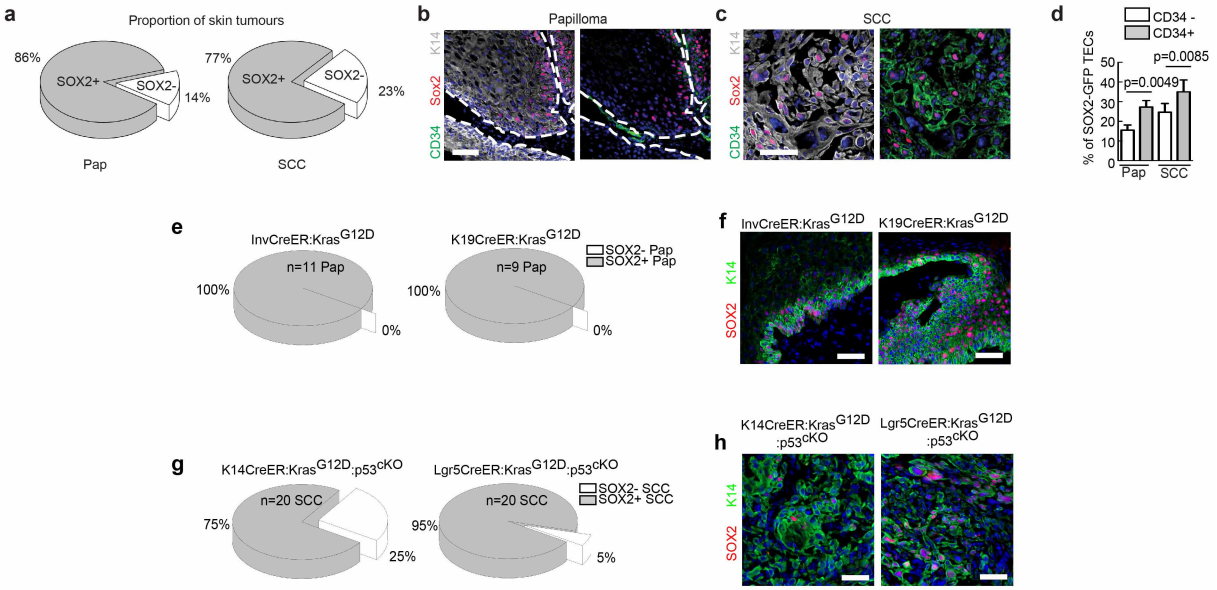

Extended Data Figure 2 | SOX2 is expressed in benign and malignant chemical-induced skin tumours and in genetically induced skin tumours from different cells of origin. **a**, Quantification of the proportion of SOX2$^+$ skin tumours assessed by immunostaining for SOX2 protein ($n \geq 6$ sections analysed from 43 papillomas and 13 SCCs). **b**, **c**, Co-immunostaining of K14 (white), CD34 (green) and SOX2 protein (red) in papilloma (**b**) and SCC (**c**), showing expression of SOX2 within CD34$^+$ K14$^+$ TECs. **d**, FACS quantification of SOX2–GFP$^+$ cells in CD34$^+$ and CD34$^-$ TECs (Lin$^-$Epcam$^+$) within benign papillomas and malignant SCCs ($n = 12$ papillomas and 26 carcinomas from at least 10 mice). **e**, Proportion of SOX2$^+$ papillomas arising from Kras(G12D) expression either in interfollicular epidermis and infundibulum (InvCreER:Kras^{G12D}) or in hair follicle stem cells and their progeny (K19CreER:Kras^{G12D}), as assessed by SOX2 immunostaining. **f**, Representative co-immunostaining of SOX2 protein (red) and K14 (green) in papilloma from InvCreER:Kras^{G12D} and K19CreER:Kras^{G12D} mice. These data show that SOX2 expression is found in papillomas arising from different epidermal origins. **g**, Proportion of SCCs containing SOX2$^+$ TECs among SCCs arising from Kras(G12D) expression and p53 deletion either in interfollicular epidermis and infundibulum cells preferentially (K14CreER:Kras^{G12D}:p53^{cKO}), or in hair follicle stem cells and their progeny (Lgr5CreER:Kras^{G12D}:p53^{cKO}). **h**, Representative co-immunostaining of SOX2 protein (red) and K14 (green) in SCCs from K14CreER:Kras^{G12D}:p53^{cKO} and Lgr5CreER:Kras^{G12D}:p53^{cKO} mice. These data show that SOX2 expression is found in SCCs from different cellular origins. Epi, tumour epithelia cells; Str, stroma. Hoechst nuclear staining is represented in blue. Scale bars, 50 μm. Data represent the mean and s.e.m.

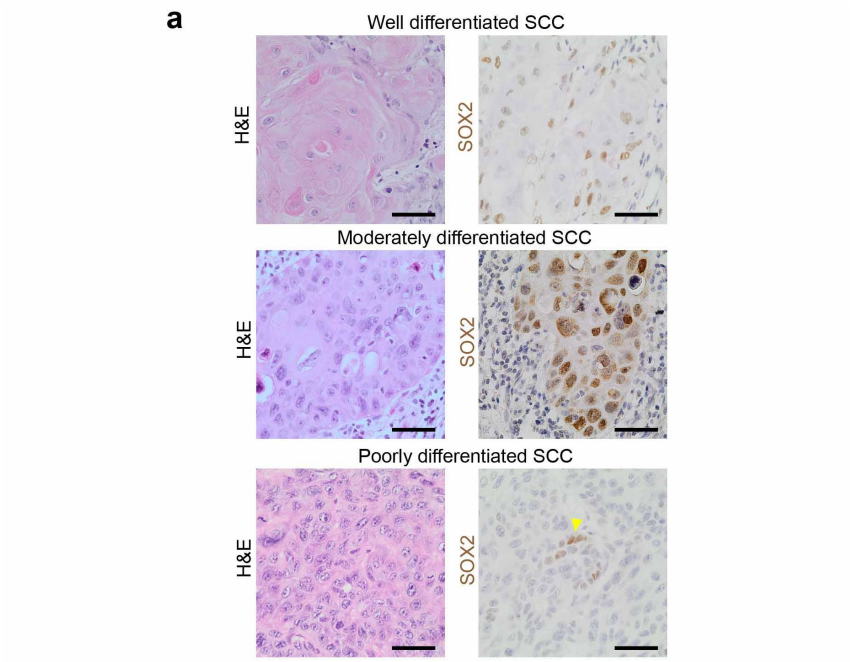

b

SOX2 expression / differentiation

Exact Fisher p=0,4793	Well+Moderately differentiated	Poorly differentiated	Total
SOX2 Positive	**17**	**7**	24
SOX2 Negative	**7**	**5**	12
Total	24	12	**36**

c

SOX2 expression / invasion

Exact Fisher p=0,691	Minimal Invasion	Large Invasion	Total
SOX2 Positive	**6**	**18**	24
SOX2 Negative	**2**	**10**	12
Total	8	28	**36**

Extended Data Figure 3 | SOX2 expression in human skin SCCs. **a**, Representative haematoxylin and eosin (H&E) staining (left) and SOX2 immunostaining (right) in well-differentiated (top), moderately (middle) and poorly (bottom) differentiated human skin SCC. **b**, Representative table of the comparison of SOX2 in well or moderately versus poorly differentiated human SCC. **c**, Representative table of the comparison of SOX2 expression in minimal invasion versus large invasion of human SCCs. Scale bars, 20 μm.

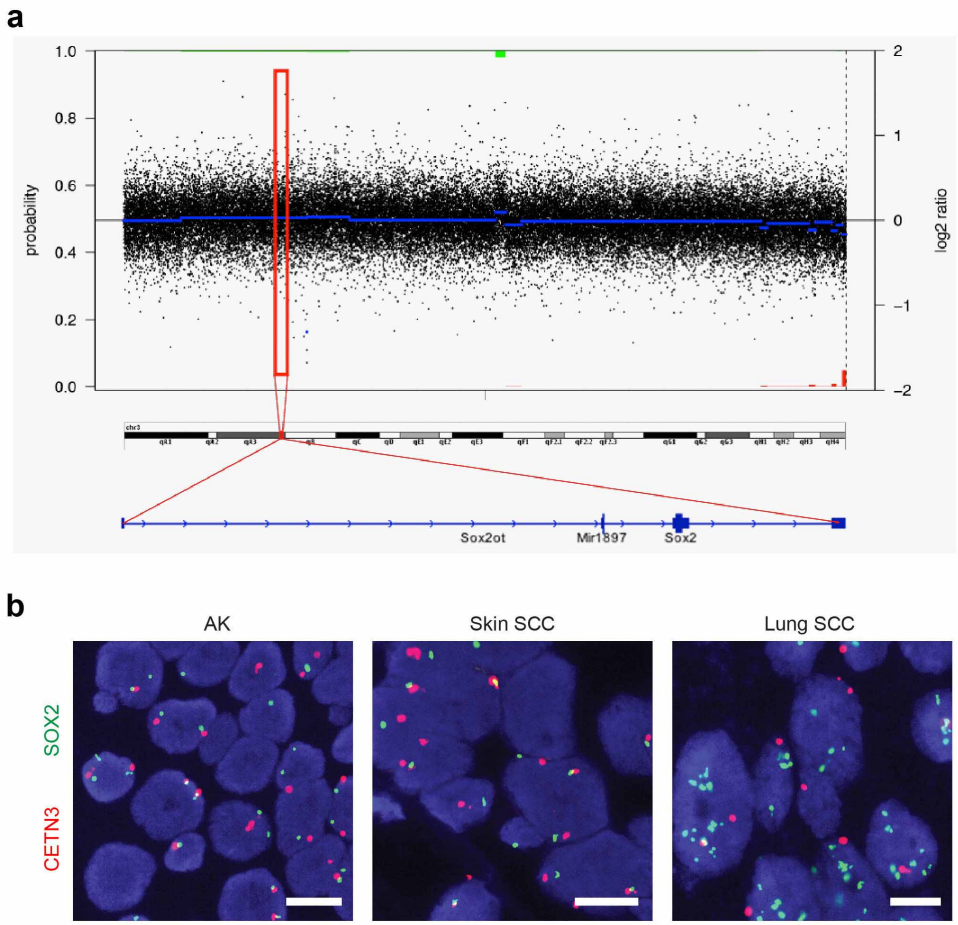

Extended Data Figure 4 | *Sox2* DNA copy number assessed in mouse and human skin SCCs. a, Comparative genomic hybridization array performed on DNA from TECs compared to their corresponding germline bone marrow DNA of the same animal. Data are segmented and normalized in relation to the intensity of their neighbouring probes to detect with high confidence genomic regions that have been amplified or deleted[42,43]. Graph plot representing an overview of the aberrations found in chromosome 3 from a representative SCC. No amplification of the genomic region containing *Sox2* (red box) is detected in TECs from invasive SCC. Horizontal blue lines represent the normalized $\log_2$ ratios of the DNA copy number of the different probes along the chromosome. Vertical bars indicate the regions with a certain probability of deletion (red) (*P*) or amplification (green) ($1 - P$). These analyses were performed on five different SCCs with similar results concerning the absence of *Sox2* deletion. **b**, FISH experiment using a green-labelled *SOX2* gene probe and an orange-labelled centromeric probe for chromosome 3 (*CETN3*) as reference probe against *SOX2* (green) performed in actinic keratosis (AK), skin SCC and lung SCC human samples. These data show that, although the *SOX2* gene is amplified in human lung SCC as previously described[7], there is no *SOX2* amplification in AK or in skin SCC. DAPI nuclear staining is represented in blue. Scale bars, 10 μm.

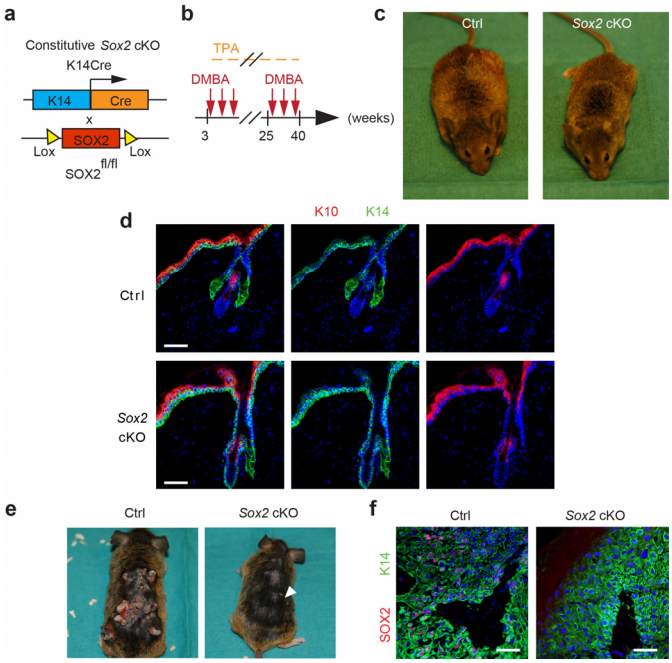

Extended Data Figure 5 | *Sox2* deletion in the epidermis does not impair skin homeostasis but markedly decreases skin tumour initiation. **a**, Genetic strategy used to study the role of SOX2 expression in tumour initiation. **b**, Protocol of repeated DMBA/TPA administration. **c**, Macroscopic pictures of control (Ctrl) and *Sox2*-deleted mice in all epidermal cells starting from embryonic development (K14Cre:SOX2$^{fl/fl}$ mice = *Sox2* conditional knockout (cKO)). **d**, Immunostaining of K14 (green) and K10 (red) in control and *Sox2* conditional knockout skin sections during adult homeostasis. These data show that *Sox2* deletion does not impair skin differentiation under physiological conditions. **e**, Pictures of control and *Sox2* conditional knockout mice following DMBA/TPA treatment. These data show that *Sox2* conditional knockout mice have a marked reduction in the number of skin tumours. **f**, Co-immunostaining of K14 (green) and SOX2 protein (red) in papillomas, showing the absence of SOX2 expression in the rare skin papillomas arising in *Sox2* conditional knockout mice. Scale bars, 50 μm.

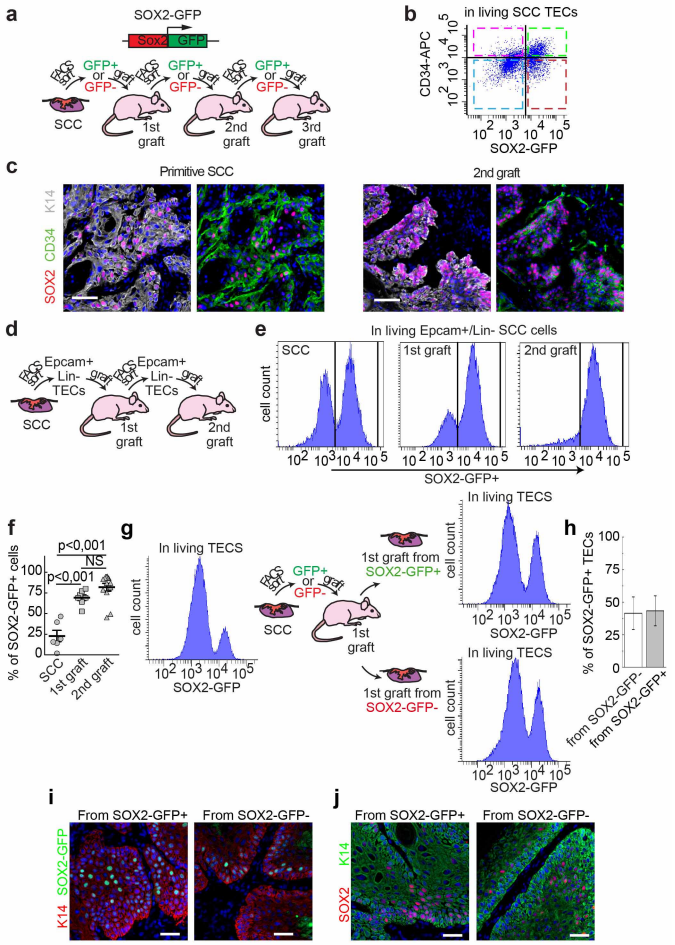

Extended Data Figure 6 | Competitive advantage of SOX2–GFP$^+$ cells and inefficient reversibility of SOX2 expression during tumour transplantation. **a**, Scheme summarizing the experimental strategy used to define the tumour-propagating capacities of SOX2–GFP$^+$ and GFP$^-$ TEC populations during serial transplantations of DMBA/TPA-induced SCCs. **b**, FACS analysis of SOX2–GFP and CD34 within the TEC population in a representative primary SCC. **c**, Co-immunostaining for K14 (white), CD34 (green) and SOX2 (red) in a primitive mouse skin SCC and tumours arising following the serial transplantation of SOX2–GFP$^+$ TECs, showing the increased proportion of cells expressing SOX2 after serial transplantation. **d**, Scheme representing the strategy used to measure enrichment of SOX2–GFP$^+$ TECs during serial transplantations. Epcam$^+$ TECs were FACS isolated from primary SCCs, primary (1st graft) and secondary grafts (2nd graft) using co-staining for Epcam and Lin$^-$. **e**, Representative FACS plots of SOX2–GFP$^+$ expression in Epcam$^+$/Lin$^-$ TECs from SCC, 1st and 2nd grafts. These data show that the proportion of SOX2–GFP$^+$ TECs increases over serial transplantation. **f**, Quantification of the proportion of SOX2–GFP$^+$ cells in TECs from primary SCCs ($n = 6$), 1st graft ($n = 7$) and 2nd graft ($n = 13$). Analysis of variance was performed ($P < 0.0001$) followed by Tukey test for comparison of each pair of conditions. **g**, Scheme representing the strategy and FACS analysis used to measure reversibility of SOX2–GFP$^+$ and SOX2–GFP$^-$ TECs upon transplantation. TECs were sorted based on SOX2–GFP expression from primary tumour (SCC) and primary (1st) graft, using co-staining for Epcam, SOX2–GFP and Lin$^-$. **h**, FACS quantification of the proportion of SOX2–GFP$^+$ cells in the primary graft from SOX2–GFP$^+$ and SOX2–GFP$^-$ tumours. ($n = 5$ tumours from 5 mice for each group). **i**, **j**, Co-immunostaining for K14 (red) and GFP (green) (**i**) and for K14 (green) and SOX2 (red) (**j**) in primary tumours arising from transplantation of SOX2–GFP$^+$ or SOX2–GFP$^-$ TECs, showing the inefficient reversibility of SOX2-negative cells into SOX2-positive cells. Hoechst nuclear staining is represented in blue. Scale bars, 50 μm. Data represent the mean and s.e.m. NS, not significant.

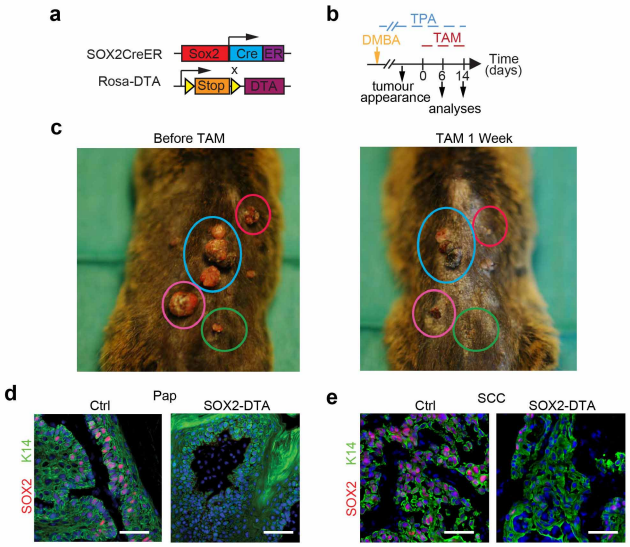

Extended Data Figure 7 | SOX2 lineage ablation in pre-existing skin tumours leads to their regression. **a**, Genetic strategy used to perform lineage ablation of SOX2-expressing cells in pre-existing tumours. **b**, Experimental design. **c**, Macroscopic pictures of skin papillomas before and after $SOX2^{+}$ cells lineage ablation. Tamoxifen (TAM) administration to SOX2CreER:Rosa-DTA mice presenting with skin tumours leads to their regression. **d**, **e**, Co-immunostaining for K14 (green) and SOX2 protein (red) in papilloma (**d**) and in carcinoma (**e**) arising from control (Ctrl) (left) and SOX2CreER:Rosa-DTA (SOX2–DTA) (right) mice. These data show efficient ablation of SOX2-expressing cells. Scale bars, 50 μm.

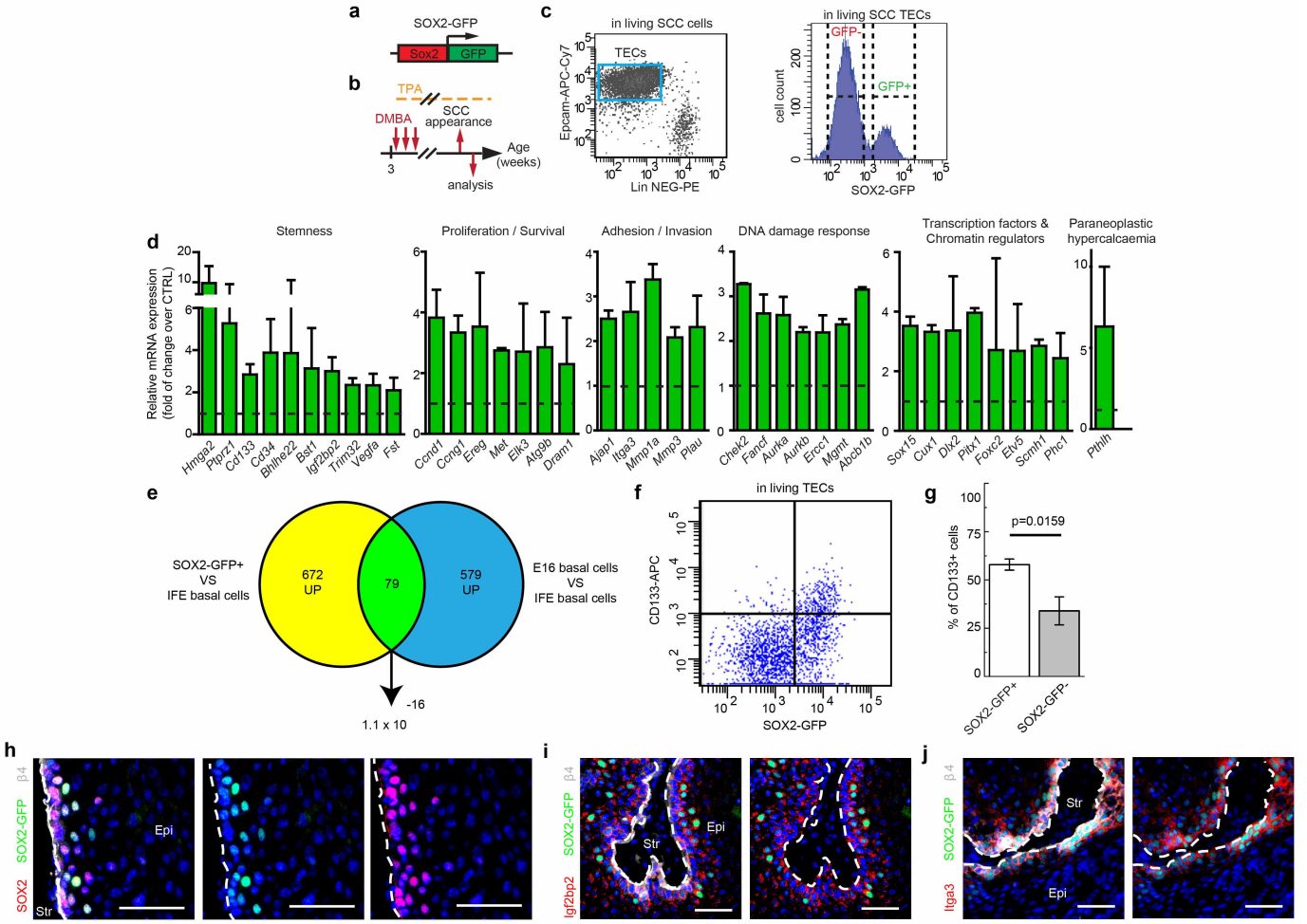

Extended Data Figure 8 | Molecular characterization of SOX2–GFP$^+$ SCC TECs. **a**, Genetic strategy used to isolate SOX2–GFP-expressing TECs by FACS. **b**, Protocol used to induce skin carcinogenesis. **c**, FACS strategy used to isolate SOX2–GFP$^+$ and SOX2–GFP$^-$ TECs. **d**, Histograms summarizing the genes upregulated in SOX2–GFP$^+$ TECs (the histograms show the mean and s.e.m. of microarray signals performed in duplicate). These data show that SOX2–GFP$^+$ TECs of SCCs preferentially express genes involved in tumour stemness, proliferation/survival, cell adhesion/invasion, transcription and chromatin remodelling factors, DNA damage response and paraneoplasic hypercalcaemia. **e**, Venn diagram showing the overlap between the genes upregulated in SOX2–GFP$^+$ TECs and the genes upregulated in wild-type E16 basal epidermal cells[49,50] as compared to adult basal epidermal cells (fold change >3). The arrow indicates the hypergeometric *P* value of this overlap. **f**, FACS analysis of SOX2–GFP and CD133 within TECs from invasive SCCs. **g**, FACS quantification of the percentage of CD133$^+$ cells in SOX2–GFP$^+$ and SOX2–GFP$^-$ SCC TECs ($n = 5$ SCCs). **h**–**j**, Co-immunostaining of β4 integrin (white), SOX2–GFP (green) and SOX2 protein (**h**) or Igf2bp2 (**i**) or Itgα3 (red) (**j**), showing the co-expression of these markers by SOX2–GFP-expressing TECs. Epi, epithelium; Str, tumour stroma. Scale bars, 50 μm. Data represent the mean and s.e.m.

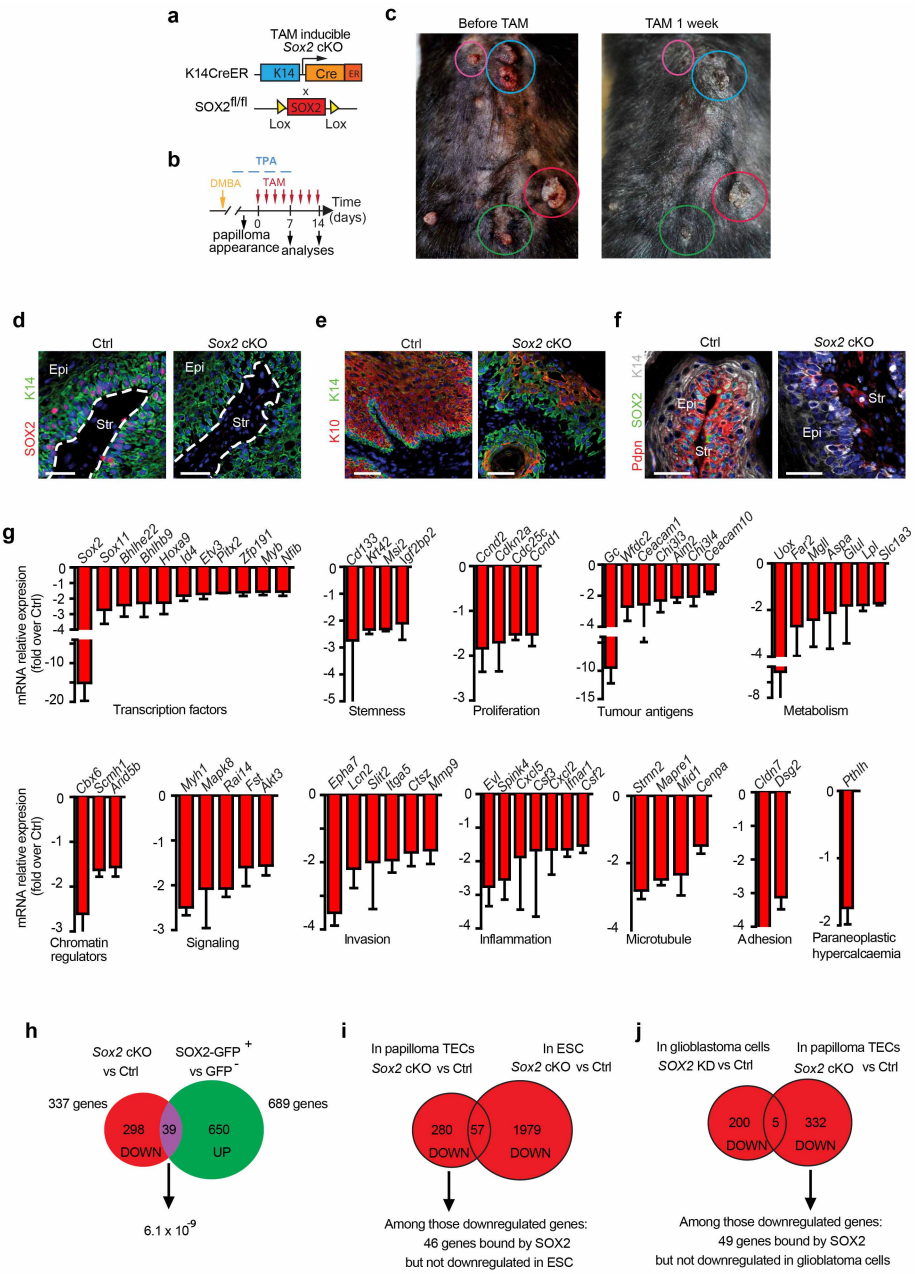

Extended Data Figure 9 | Functional and molecular characterization of skin papillomas after *Sox2* deletion. **a**, Genetic strategy used to study the role of SOX2 in pre-established skin tumours. **b**, Protocol of DMBA/TPA and tamoxifen (TAM) administration. **c**, Macroscopic pictures of skin papillomas after *Sox2* deletion. Tamoxifen administration to K14CreER:SOX2$^{fl/fl}$ mice presenting with skin papillomas leads to their regression. **d**, Co-immunostaining for K14 (green) and SOX2 protein (red) in control (Ctrl) and *Sox2* conditional knockout (cKO) papilloma after 1 week of tamoxifen administration showing the disappearance of SOX2 expression in the tamoxifen-treated conditions. **e**, Co-immunostaining for K14 (green) and K10 (red) in control and *Sox2* conditional knockout papilloma after 1 week of tamoxifen administration showing the decrease in the number of differentiated K10^{+} cells in *Sox2* conditional knockout tumours. **f**, Co-immunostaining for K14 (white), Pdpn (red) and SOX2 protein (green) in control and *Sox2* conditional knockout papilloma after 1 week of tamoxifen administration. **g**, Histograms summarizing the genes downregulated in *Sox2* conditional knockout TECs of papillomas ($n = 3$ microarrays for each group and the histograms show the mean and s.e.m.). These data show that SOX2 controls a gene network that regulates tumour stemness, proliferation/survival, metabolism, cell adhesion/invasion, transcription and chromatin remodelling factors, and paraneoplastic hypercalcaemia. **h**, Venn diagram showing the overlap between the genes upregulated in the SOX2^{+} CSC signature and downregulated following *Sox2* deletion. The arrow indicates the hypergeometric *P* value of this overlap. These data show that genes preferentially expressed by SOX2–GFP^{+} CSCs and positively controlled by SOX2 are significantly enriched. Genes of this overlap are presented in Supplementary Table 1. **i**, Venn diagram showing the overlap between the genes downregulated following SOX2 deletion in skin TECs and downregulated in inducible *Sox2*-null mouse embryonic stem cells (*Sox2* cKO)[27]. The 57 genes of the overlap and the 46 genes downregulated in the SOX2-regulated gene signature and bound by SOX2 in embryonic stem cells[28] are presented in Supplementary Table 2. **j**, Venn diagram showing the overlap between the genes downregulated in the SOX2-regulated gene signature and genes downregulated (fold change >2) in a transient knockdown of *SOX2* in a human glioblastoma cell line (*SOX2* KD)[29]. The 5 genes of the overlap and the 49 genes downregulated in the SOX2-regulated gene signature and bound by SOX2 in the human glioblastoma cell line are presented in Supplementary Table 3. Scale bars, 50μm. Down, downregulated genes; Epi, epithelium; ESC, embryonic stem cells; GB, glioblastoma cell line; Str, stroma; Up, upregulated genes.

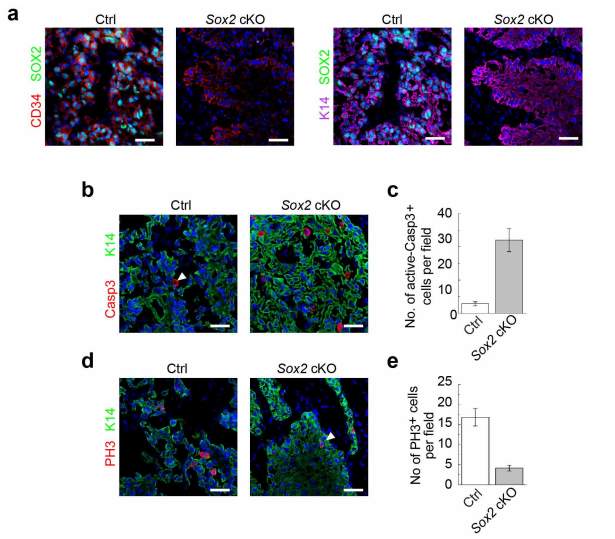

Extended Data Figure 10 | Functional characterization of skin SCCs following SOX2 deletion. **a**, Co-immunostaining for SOX2 protein (green) and CD34 (red) or K14 (purple) in control (Ctrl) (left) and *Sox2* conditional knockout (cKO; right) SCCs after 2 weeks of tamoxifen administration. **b**, Co-immunostaining for K14 (green) and caspase 3 (red) in control (left) and *Sox2* conditional knockout (right) SCCs after 2 weeks of tamoxifen administration. **c**, Quantification of the caspase-3-positive cells in the control and *Sox2* conditional knockout SCCs showing the increase of apoptosis in the *Sox2* conditional knockout SCCs ($n = 5$ SCCs from 4 different mice). **d**, Co-immunostaining for K14 (green) and PH3 (red) in control (left) and *Sox2* conditional knockout (right) SCCs after 2 weeks of tamoxifen administration. **e**, Quantification of PH3-positive cells in control and *Sox2* conditional knockout SCCs showing the decrease of proliferation in *Sox2* conditional knockout SCCs ($n = 5$ SCCs from 4 different mice). Scale bars, 50 μm. Data represent the mean and s.e.m.